Quaternary Research (2018), **90**, 331–347.

doi:10.1017/qua.2018.47

Loess–paleosol carbonate clumped isotope record of late Pleistocene–Holocene climate change in the Palouse region, Washington State, USA

Alex R. Lechler[a]*, Katharine W. Huntington[b], Daniel O. Breecker[c], Mark R. Sweeney[d], Andrew J. Schauer[b]

[a]Department of Geosciences, Pacific Lutheran University, Tacoma, Washington 98447, USA
[b]Department of Earth and Space Sciences, University of Washington, Seattle, Washington 98195, USA
[c]Department of Geological Sciences, Jackson School of Geosciences, University of Texas at Austin, Austin, Texas 78712, USA
[d]Department of Sustainability and Environment, University of South Dakota, Vermillion, South Dakota 57069, USA

(Received October 17, 2017; Accepted April 9, 2018)

Abstract

The Channeled Scabland–Palouse region of the Pacific Northwest (PNW) of the United States preserves geomorphic and pedosedimentary records that inform understanding of late Pleistocene–Holocene paleoclimate change in a region proximal to the last glacial period Cordilleran Ice Sheet. We present a clumped (Δ_{47}) and conventional ($\delta^{18}O$, $\delta^{13}C$) isotopic study of Palouse loess–paleosol carbonates in combination with carbonate radiocarbon (^{14}C) dating to provide new measures of regional late–last glacial (~31–20 cal ka BP) and Holocene soil conditions. Average clumped isotope temperatures ($T(\Delta_{47})$) for last glacial Palouse loess–paleosol carbonates (9 ± 4°C) are significantly lower than those for Holocene-aged carbonates ($T(\Delta_{47}) = 18 \pm 2$°C) in study sections. Calculated soil water $\delta^{18}O_{VSMOW}$ values (-16 ± 2‰) for last glacial carbonates are also offset relative to those for Holocene-aged samples (-11 ± 1‰), whereas calculated soil CO_2 $\delta^{13}C_{VPDB}$ values are similar for the Holocene (-16.9 ± 0.2‰) and late–last glacial (-16.7 ± 1.1‰) periods. Together, these paleoclimate metrics indicate late–last glacial conditions of pedogenic carbonate formation in the C_3 grassland soils of the Palouse were measurably colder (9 ± 5°C) than during the Holocene and potentially reflect a more arid last glacial paleoclimate across the Palouse, findings in agreement with previous proxy studies and climate model simulations for the region.

Keywords: Loess; Paleosol; Palouse; Clumped isotope; Pedogenic carbonate; LGM, Paleoclimate

INTRODUCTION

Proxy-based quantifications of late Pleistocene and, specifically, last glacial maximum (LGM; ~23–19 ka BP; Mix et al., 2001) paleoclimate conditions are fundamental to assessing and refining climate model simulations of past and future climate states with varied atmospheric pCO_2. Marine proxy records (e.g., MARGO Project Members, 2009) have proven effective for LGM proxy-model comparisons (Otto-Bliesner et al., 2009; Hargreaves et al., 2011; Schmittner et al., 2011; Annan and Hargreaves, 2013, 2015) due to their relative completeness and coherence. In comparison, LGM model benchmarking with terrestrial proxy records (e.g., Bartlein et al., 2011) is inherently more challenging due to enhanced climate sensitivity in terrestrial settings (i.e., land–sea contrast; Braconnot et al., 2012; Annan and Hargreaves, 2013, 2015; Harrison et al., 2015) and the relative incompleteness and lower preservation potential for terrestrial deposits. As a result, there is an ever-present need for new and robust quantitative records of terrestrial paleoclimate.

The Channeled Scabland–Palouse region of Washington State (USA) (Fig. 1A) preserves a rich geomorphic, sedimentological, and pedogenic record of late Pleistocene terrestrial paleoclimate and last glacial–interglacial climate change. Nearly a century of research has clarified links between late Pleistocene climate change and Cordilleran Ice Sheet growth/retreat cycles, glacial-outburst megafloods, and Palouse loess–paleosol development (Bretz, 1923, 1969; Baker and Bunker, 1985; Waitt, 1985; Busacca, 1989; Baker et al., 1991; McDonald and Busacca, 1990, 1992; O'Connor and Baker, 1992; Busacca and McDonald, 1994; Richardson et al., 1997; Clague et al., 2003; Gaylord et al., 2003;

*Corresponding author at: Department of Geosciences, Pacific Lutheran University, Rieke 158, Tacoma, Washington 98447, USA. E-mail address: Lechlear@plu.edu (A.R. Lechler).

Sweeney et al., 2004, 2005, 2007; Pluhar et al., 2006; Baker, 2009; Hanson et al., 2012; McDonald et al., 2012; Bader et al., 2016). Covering ~50,000 km^2 of the Columbia Plateau (Fig. 1A) and being up to ~75 m thick in places (McDonald et al., 2012), the Palouse loess, in particular, preserves a protracted history of Quaternary climate change in the Pacific Northwest (PNW).

As the ultimate product of late Pleistocene megafloods that sculpted the Channeled Scabland of the PNW (e.g., Baker, 2009; Baker et al., 2016), the Palouse loess was a sensitive recorder of regional late Pleistocene climate fluctuations. Periods of loess accumulation occurred during and immediately following times of increased megaflood frequency associated with ice sheet retreat; these megafloods delivered sediments to slackwater depocenters along the Columbia River in SE Washington and NE Oregon that were subsequently entrained by prevailing southwesterly winds and deposited across the Palouse (Busacca and McDonald, 1994; Sweeney et al., 2007; McDonald et al., 2012; Fig. 1A). Under peak glacial conditions, anticyclonic winds developed over the Laurentide Ice Sheet appear to have effectively shut down loess-transporting winds, leading to periods of reduced loess accumulation and more sustained pedogenic development across the Palouse (Sweeney et al., 2004; Fig. 1A). The resulting Palouse loess–paleosol sequences (Fig. 1B) thus preserve a record of the alternating periods of ice sheet growth and retreat that characterized North America throughout the Late Quaternary.

Loess–paleosols developed throughout the late last glacial period (~35–15 ka; Sweeney et al., 2004) and early Holocene are well preserved across the Palouse, making them valuable pedosedimentary archives of regional last glacial–Holocene terrestrial climate change. Here we present the first clumped isotope temperature records from Palouse loess–paleosol carbonates in combination with new carbonate stable-isotope analyses ($\delta^{18}O$, $\delta^{13}C$) and radiocarbon (^{14}C) ages to provide insight into the magnitudes and character of late Pleistocene–Holocene climate change in a terrestrial region proximal to the Cordilleran Ice Sheet (Fig. 1A).

Background

Modern climate and soils of the Palouse

The modern Palouse is a winter precipitation–dominated, C_3 grassland in the rain shadow of the Cascades Range. Mean annual temperature (MAT) and precipitation (MAP) vary with elevation across the region. MAT ranges from ~12°C at low-elevation (<500 m asl) sites in the westernmost Palouse to 6°C at elevations >1500 m asl in the Blue Mountains of southeast Washington. Modern soil types transition with climate across the Palouse with Aridisols in the west (MAP < 230 mm), Mollisols in steppe/meadow steppe (MAP = 230–600 mm) environments in the central Palouse, and Alfisols/Andisols in higher-elevation forest settings to the east (MAP > 600 mm; Boling et al., 1998).

Modern precipitation $\delta^{18}O$ values in the Palouse vary seasonally, higher (−8‰ to −14‰ Vienna Standard Mean Ocean Water [VSMOW]) in the warm season (April–September) than during the winter (−11‰ to −17‰), with weighted mean annual $\delta^{18}O$ values of −13‰ to −14‰ (Takeuchi et al., 2009). Regional soil waters ($\delta^{18}O$ ~ −12‰ to −16‰; Takeuchi et al., 2009) generally reflect the dominance of cool-season precipitation in the region but can be impacted by significant evaporative ^{18}O enrichment at shallow-soil depths (Stevenson et al., 2010).

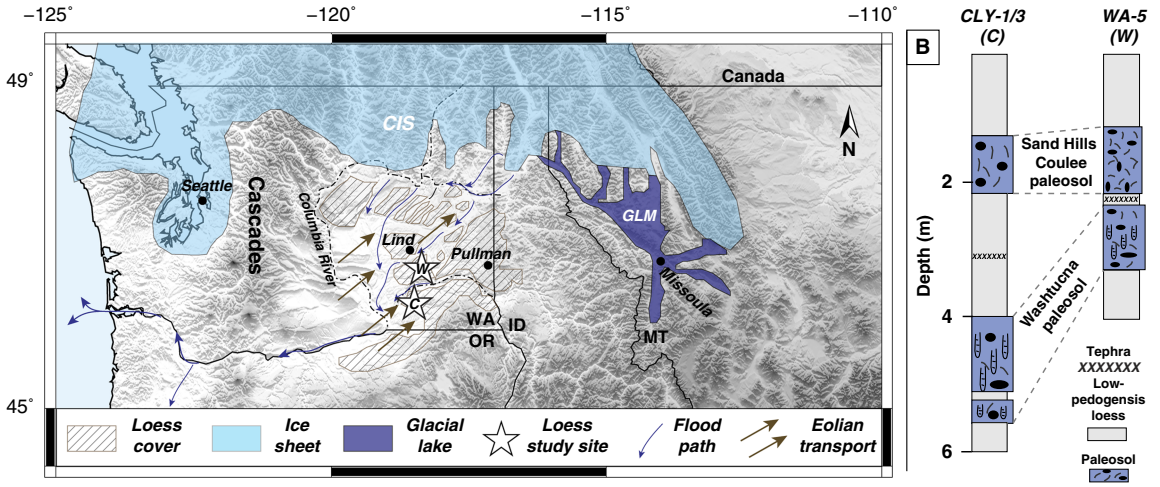

Figure 1. (color online) Study area during the late glacial period. (A) Last glacial period map of the greater Palouse region imposed on modern shaded-relief digital elevation model. Cordilleran Ice Sheet (CIS) and Glacial Lake Missoula (GLM) extents shown are average positions throughout the late–last glacial period (~35–15 ka). Approximate megaflood paths from McDonald et al. (2012). Loess study sites marked by stars (C, CLY-1/3; W, WA-5). Lind, Soil Climate Analysis Network soil-monitoring site in Lind, WA. (B) Loess–paleosol study sections (see A for locations). CLY-1/3 refers to a combined CLY-1 and CLY-3 stratigraphic section (individual sections ~200 m apart) using the base of the Washtucna paleosol as a stratigraphic tie point. Sand Hills Coulee and Washtucna paleosol intervals preserved in each section.

https://doi.org/10.1017/qua.2018.47 Published online by Cambridge University Press

Paleoclimate setting and records

There is abundant evidence for ice sheets extending into and covering parts of the PNW throughout the last glacial period (e.g., Booth et al., 2003; Clague, 2009; Fig. 1A). Additional constraints on the last glacial climate history of the region come from lake and loess–paleosol records and general circulation model (GCM) simulations. Together, these studies suggest a measurably colder and more arid regional paleoclimate across the Palouse during the LGM.

LGM GCM simulations (Kutzbach and Wright, 1985; COHMAP Members, 1988; Bartlein et al., 1998; Whitlock et al., 2001; Bromwich et al., 2004, 2005) and ensemble studies (Braconnot et al., 2012; Annan and Hargreaves 2013, 2015) show magnitudes of regional LGM cooling in excess of 15°C across the interior of the Laurentide–Cordilleran Ice Sheet, significantly greater than the average global LGM–Holocene temperature change of ~4°C (Annan and Hargreaves 2013, 2015). Such amplification appears to have led to pronounced meridional temperature gradients near the southern margin of the Cordilleran Ice Sheet (Schmittner et al., 2011; Annan and Hargreaves, 2013, 2015), with simulations showing LGM cooling across the Palouse region of 5–15°C (Paleoclimate Modeling Intercomparison Project [PMIP3], https://pmip3.lsce.ipsl.fr [accessed October 15, 2017]).

Phytolith records preserved in Palouse loess (Blinnikov et al., 2001, 2002) and pollen records from Carp Lake in the western Columbia Plateau (Barnosky, 1985; Thompson et al., 1993; Whitlock and Bartlein, 1997) provide additional information about late Pleistocene-to-Holocene climate and vegetation change and support interpretations of measurably colder and drier LGM climate across the region. Estimates of LGM MAT and MAP derived from these records (Whitlock and Bartlein, 1997; Blinnikov et al., 2002) generally agree with magnitudes of GCM-simulated MAT cooling (4–8°C) and MAP decrease (on the order of 500–1000 mm/yr) for the greater Palouse region during the LGM (Bartlein et al., 2011). However, quantifying LGM MAT/MAP using such paleovegetation proxy records is limited by uncertainties inherent to the modern analog approaches used to derive paleo-MAT and paleo-MAP values (Bartlein et al., 2011, and references therein) and by the fact that reduced pCO_2 during the LGM (~190 ppm; Monnin et al., 2001) likely impacted regional paleovegetation independent from and/or in addition to MAT/MAP-induced changes (Braconnot et al., 2012).

Palouse loess–paleosol sequences have also been subject to prior carbonate stable isotopic study (Takeuchi et al., 2009; Stevenson et al., 2005, 2010). On the basis of higher $\delta^{18}O$ and $\delta^{13}C$ values for presumed last glacial period carbonates in comparison to those from Holocene intervals, Takeuchi et al. (2009) presented an interpretation of a colder, drier, and seasonally distinct (drier winters) LGM paleoclimate across the Palouse. However, the authors noted the difficulty in quantifying paleotemperature and paleoprecipitation values on the basis of pedogenic carbonate (PC) $\delta^{18}O$ alone, because unconstrained values for paleosoil temperature and water $\delta^{18}O$ both impact carbonate $\delta^{18}O$.

Carbonate clumped isotope thermometry

Independent temperature constraints from carbonate clumped isotope thermometry can further clarify paleoenvironmental reconstruction from Palouse proxy records. Clumped isotope thermometry (Schauble et al., 2006; Ghosh et al., 2006; Eiler, 2011) has been applied across a spectrum of earth science subdisciplines, from tectonics and structural diagenesis applications (for review, see Huntington and Lechler, 2015) to paleoclimate studies in both terrestrial and marine realms (for reviews, see Eiler, 2007, 2011; Affek, 2012; Passey, 2012). The method uses the thermodynamically driven increase in the abundance of ^{13}C-^{18}O bonds in the carbonate crystal lattice with decreasing mineral formation temperatures (Schauble et al., 2006; Ghosh et al., 2006; Eiler, 2011). The abundance of "clumped" ^{13}C-^{18}O bonds in a carbonate sample relative to the abundance that would be expected for the random distribution of isotopes is measured with high-precision mass spectrometry and quantified as the Δ_{47} parameter, where "47" refers to measurements of mass-47 CO_2 (mostly clumped $^{13}C^{18}O^{16}O$) gas produced from phosphoric acid digestion of the carbonate sample.

As a direct and quantitative measure of carbonate formation temperature, $T(\Delta_{47})$ offers valuable (paleo)climate information on its own. When combined with carbonate $\delta^{18}O$ and $\delta^{13}C$ measurements, $T(\Delta_{47})$ also allows for direct calculation of water $\delta^{18}O$ and CO_2 $\delta^{13}C$ for the aqueous solution from which carbonates precipitated. Accordingly, application of carbonate clumped isotope thermometry extends the potential for loess–paleosol proxy records to contribute to mechanistic understandings of Late Quaternary climate variability (e.g., Eagle et al., 2013).

SAMPLING AND ANALYTICAL METHODS

Loess–paleosol study sections and sampling strategy

The most recent phase of late Pleistocene megafloods occurred as climate transitioned from the LGM into the present interglacial (~15.3–12.7 ^{14}C cal ka BP; Waitt, 1985). Mount St. Helens (MSH) set S tephras commonly preserved at the base of the associated loess sequence (L1 loess of McDonald and Busacca, 1992) indicate a maximum depositional age of ~16 ka for the interval (Clynne et al., 2008). Also contained within L1 loess is the Sand Hills Coulee (SHC) paleosol, a weakly developed paleosol characterized by filamentous soil carbonate and sparse cylindrical burrows (McDonald and Busacca, 1992). Age of SHC soil development is uncertain, but its stratigraphic position within L1 loess suggests formation during the latest Pleistocene–early Holocene (McDonald and Busacca, 1992; Sweeney et al., 2005). Marking the boundary between L1 and underlying L2 loess across much of the Palouse is the prominent Washtucna paleosol, an identifiable interval highly indurated with calcium carbonate and characterized by cylindrical soil fabric

https://doi.org/10.1017/qua.2018.47 Published online by Cambridge University Press

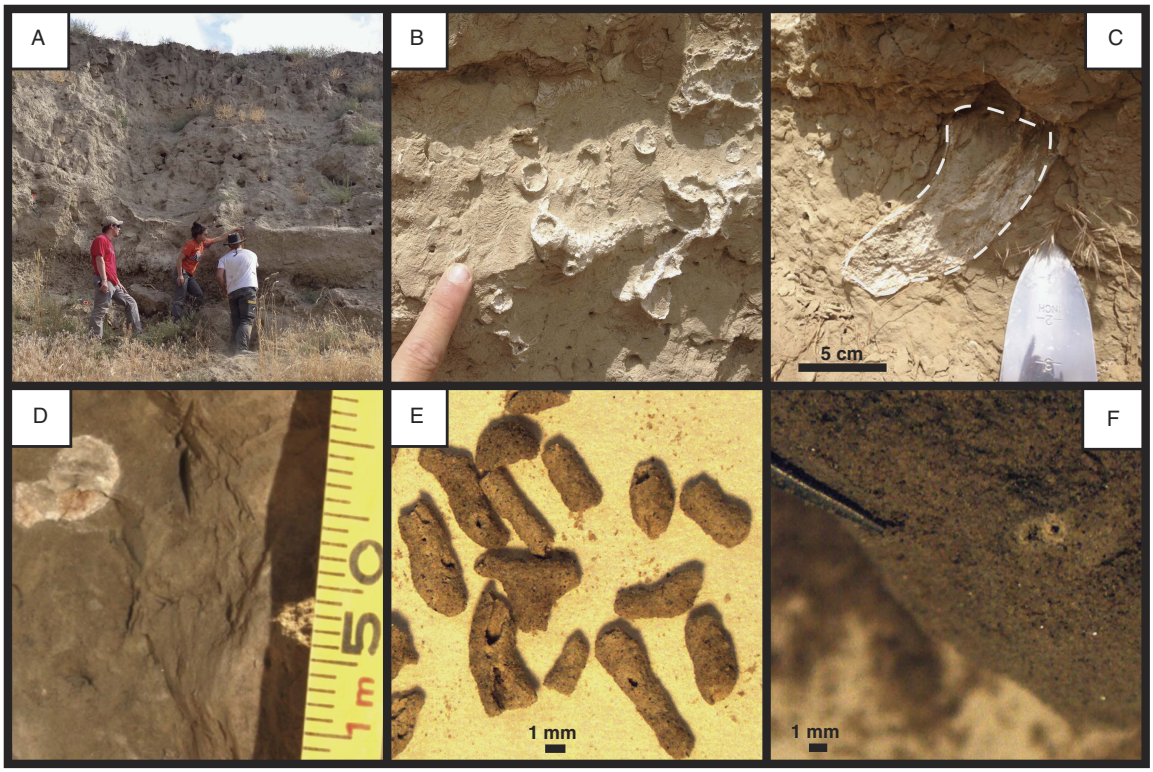

Figure 2. (color online) High-$CaCO_3$-density macroscopic PC targets for clumped and isotopic analysis. (A) CLY-1 roadcut. Student researchers (~1.7 m tall) measuring thickness of carbonate-rich, bifurcated Washtucna paleosol interval. (B) Carbonate burrow fills within Washtucna paleosol at CLY-1. (C) Rhizolith complex in Washtucna paleosol (outlined with dashed line; sample CLY1_-15). (D) A 1-cm-diameter rhizolith (sample WA5_290295). Carbonate root-pore cements (sample WA5_122130p) shown picked (E) and in situ (F).

interpreted as a product of cicada burrows (O'Geen and Busacca, 2001; Fig. 2B). Early thermoluminescence (TL) studies of loess and MSH tephras contained within the L2 sequence suggest L2 loess was deposited between latest Marine Isotope Stage (MIS) 4 and latest MIS 2 (~70 and 15 ka, respectively; Berger and Busacca, 1995; Richardson et al., 1997); within this interval; TL ages of 40 and 20 ka bracket the Washtucna paleosol (Richardson et al., 1997).

For this study, we present conventional ($\delta^{18}O$, $\delta^{13}C$) and clumped (Δ_{47}) isotopic analyses and new radiocarbon data for loess–paleosol carbonates from two Palouse sections, CLY-1/3 (46.31348°N, 118.48927°W) and WA-5 (46.77343°N, 118.35604°W; Fig. 1), that have been subject to prior stratigraphic and isotopic study (McDonald and Busacca, 1990, 1992; Sweeney et al., 2004; Takeuchi et al., 2009; McDonald et al., 2012). Both CLY-1/3 and WA-5 study sections are characterized by loess with intervals of weak pedogenesis alternating with $CaCO_3$-cemented paleosols. SW-to-NE eolian transport of Palouse loess from megaflood depocenters along the Washington–Oregon border (Fig. 1A) resulted in downwind fining and thinning of Palouse loess sequences (Sweeney et al., 2005; McDonald et al., 2012). As a result, the more proximal (<20 km from loess source) CLY-1/3 section is significantly thicker than the downwind WA-5 site (~60 km from source). L1 and L2 loess at CLY-1/3 are ~4.5 and 9 m thick, respectively, in comparison to 2 m (L1) and 2.5 m (L2) at WA-5 (McDonald et al., 2012). The SHC and Washtucna paleosols are preserved in each study section, with the Washtucna soil being thicker and bifurcated at the CLY site (Figs. 1B and 2A).

Carbonate content varies with the degree of pedogenic development in Palouse loess–paleosol sequences, increasing from ~2 wt% $CaCO_3$ in loess intervals that have experienced minimal pedogenesis to ≥10 wt% $CaCO_3$ in well-developed paleosols like the Washtucna paleosol (McDonald and Busacca, 1992). Locally, and particularly widespread throughout the Washtucna paleosol, carbonate burrow fills and rhizoliths with >25 wt% $CaCO_3$ (hereafter referred to as "macroscopic PCs"; Fig. 2) are present. Given the potential for detrital carbonate in the loess matrix (measured at 2–8 wt % in Palouse loess sequences lacking identifiable pedogenesis; Baker et al., 1991), macroscopic PCs that are demonstrably pedogenic in origin were targeted for sampling where present.

Loess matrix samples were collected from study sections in ~5-cm-thick intervals at ~10-cm-depth spacing from the top of the shallowest (youngest) carbonate-bearing horizon down through the Washtucna paleosol, which corresponds to modern depths of 1.3–6.3 m and 0.8–4 m at CLY-1/3 and WA-5, respectively. At CLY-1/3, the shallowest sampled interval is a Bk horizon with incipient carbonate formation presumed to be Holocene in age. At WA-5, the shallowest

https://doi.org/10.1017/qua.2018.47 Published online by Cambridge University Press

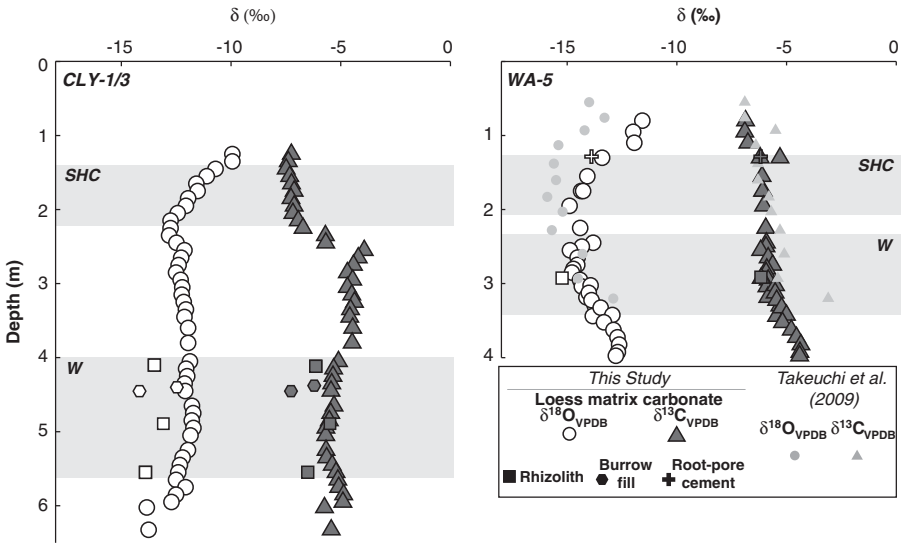

Figure 3. Carbonate $\delta^{18}O$ and $\delta^{13}C$ records for CLY-1/3 and WA-5 study sections. WA-5 isotopic data of Takeuchi et al. (2009) shown for reference. Macroscopic PCs (rhizoliths, burrow fills, root-pore cements; see Fig. 2) denoted by different symbols. SHC, Sand Hills Coulee paleosol; W, Washtucna paleosol.

sampled interval has been identified as a Bk horizon with uncertain age (McDonald and Busacca, 1990).

Carbonate Δ_{47}, $\delta^{18}O$, $\delta^{13}C$, and ^{14}C analysis

For sampled intervals at CLY-1/3 and WA-5, we measured carbonate $\delta^{18}O$ and $\delta^{13}C$ values for 83 aliquots of loess soil carbonate (Fig. 3); sample subsets (Table 1) were chosen for clumped (n = 32) and radiocarbon (n = 25) analysis to target carbonate-rich paleosol intervals (e.g., Washtucna paleosol) as well as samples characterized by endmember (i.e., maximum and minimum) carbonate $\delta^{18}O$-$\delta^{13}C$ values. Carbonate in the loess matrix is widely disseminated (3–12 wt%; Table 1) in the form of submillimeter aggregrates and loess grain coatings. As a result, loess matrix carbonate was analyzed unmodified (i.e., without physical or chemical separation from noncarbonate loess) with no cleaning or pretreatment. Macroscopic PCs were isolated from matrix loess via hand picking (root-pore cements; Fig. 2E and F) and light brushing and cleaning of carbonate burrow fills and rhizoliths (Fig. 2B, C, and D).

Carbonate Δ_{47}, $\delta^{18}O$, and $\delta^{13}C$ values were measured at the University of Washington IsoLab. Carbonate $\delta^{18}O$ and $\delta^{13}C$ values were measured using a Kiel III carbonate device coupled to a dual-inlet Finnigan Delta Plus mass spectrometer using the methods of Tobin et al. (2011). Measured isotope ratios were converted to the Vienna Pee Dee Belemnite (VPDB) and VSMOW reference scales using internal laboratory standards calibrated against NBS-18 and NBS-19 (International Atomic Energy Agency, Vienna, Austria) and LSVEC (National Institute of Standards and Technology, Gaithersburg, MD, USA) international standards, which were analyzed along with the samples.

Sample preparation for clumped isotope analysis followed the methods of Burgener et al. (2016). In brief, for each sample, an appropriate mass containing ~8 mg of $CaCO_3$ was reacted for 10 minutes in a common phosphoric acid bath held at 90°C. To separate out water, the liberated CO_2 gas was cryogenically purified through a sequence of ethanol–dry ice (~ −80°C) and liquid nitrogen traps. The CO_2 was subsequently entrained in helium and passed through a Porapaq Q column (50/80 mesh, 15 cm long, 4.5 mm ID, 0.635 mm OD) held between −10°C and −20°C. Purified CO_2 was then analyzed on a dual-inlet Thermo MAT 253 configured to measure m/Z 44-49.

Carbonate Δ_{47} values were calculated from mass spectrometer data based on Huntington et al. (2009), but using the pressure baseline (He et al., 2012) measurement, data reduction, and ^{17}O correction methods and scripts of Schauer et al. (2016). The Δ_{47} values (Table 1) were placed in the absolute reference frame (Dennis et al., 2011) using CO_2 gases heated (1000°C) or equilibrated to 4°C and 60°C.

All samples analyzed for Δ_{47} were subject to triplicate analysis at minimum (175 total Δ_{47} analyses; Table 1), with the exception of one small rhizolith sample (CLY1_-80), which provided enough carbonate for only two replicates. Pierce outlier tests (Ross, 2003) were applied to identify replicate outliers (14 of 175 Δ_{47} analyses [8%] identified as outliers), following which mean Δ_{47} and standard error (SE) of the mean values were calculated. Reported clumped isotope temperature ($T(\Delta_{47})$) values (Table 1) were calculated from mean Δ_{47} values using the empirical calibration of Kelson et al. (2017), which is based on data produced in the same laboratory and using the same ^{17}O correction as our samples.

Palouse carbonate $T(\Delta_{47})$ values reported in Table 1 are interpreted as measures of the equilibrium temperature of carbonate formation in Palouse (paleo)soils. $\delta^{18}O$ values of soil water in equilibrium with carbonate during the time of formation were calculated using measured $T(\Delta_{47})$ and

https://doi.org/10.1017/qua.2018.47 Published online by Cambridge University Press

Table 1. Clumped and Isotopic Data for Palouse study sections.

				Carbonate						*Soil CO_2*	*Water*
Sample ID	Depth (m)	n	Raw ^{14}C age ± 1σ (ka)	Calibrated ^{14}C age (cal ka BP) [*]	$CaCO_3$ (wt %)	$\delta^{13}C$ (VPDB)	$\delta^{18}O$ (VPBD)	$\Delta_{47} \pm 1$ S.E. (‰) [**]	$T(\Delta_{47}) \pm 1$ S.E. (°C) [§]	$\delta^{13}C_{VPDB}$ [+]	$\delta^{18}O_{VSMOW}$ [‡]
CLY-1/3 section											
CLY3_135140	1.38	3	–	–	4	-7.4	-9.9	0.626 ± 0.011	19 ± 3	-16.9 ± 0.4	-10.3 ± 0.7
CLY3_155160	1.58	4	8.0 ± 0.1	8.8 ± 0.2	9	-7.3	-11.1	0.631 ± 0.010	18 ± 3	-17.0 ± 0.3	-11.8 ± 0.6
CLY3_175180	1.78	4	9.7 ± 0.1	11.1 ± 0.2	6	-7.1	-11.5	0.628 ± 0.010	19 ± 3	-16.7 ± 0.3	-12.0 ± 0.6
CLY3_205210	2.08	4	11.0 ± 0.1	12.9 ± 0.2	6	-7.2	-12.4	0.636 ± 0.010	16 ± 3	-17.0 ± 0.3	-13.4 ± 0.6
CLY3_235240	2.38	4	16.6 ± 0.1	20 ± 0.2	6	-5.7	-12.8	0.572 ± 0.010	37 ± 3	-13.1 ± 0.4	-9.8 ± 0.6
CLY3_255260	2.58	9	20.0 ± 0.1	24.1 ± 0.2	8	-3.9	-12.1	0.558 ± 0.017	42 ± 7	-10.7 ± 0.8	-8.3 ± 1.2
CLY3_290295	2.93	6	20.4 ± 0.2	24.5 ± 0.4	8	-3.9	-12.1	0.580 ± 0.019	34 ± 7	-11.7 ± 0.8	-9.7 ± 1.3
CLY3_345350	3.48	4	20.0 ± 0.1	24.1 ± 0.2	6	-4.6	-12.1	0.568 ± 0.011	39 ± 4	-11.8 ± 0.5	-8.9 ± 0.7
CLY3_405410	4.08	4	–	–	5	-5.1	-11.9	0.612 ± 0.010	24 ± 3	-14.1 ± 0.4	-11.4 ± 0.6
CLY1_-160	*4.10*	*7*	*17.4 ± 0.1*	*21.1 ± 0.3*	*50*	*-6.1*	*-13.5*	*0.658 ± 0.007*	*10 ± 2*	*-16.7 ± 0.2*	*-15.8 ± 0.4*
CLY1_-125	*4.45*	*4*	*25.5 ± 0.2*	*29.6 ± 0.4*	*27*	*-7.2*	*-14.2*	*0.693 ± 0.010*	*1 ± 2*	*-18.8 ± 0.3*	*-18.5 ± 0.6*
CLY3_445450	4.48	5	20.0 ± 0.1	24.1 ± 0.3	5	-5.4	-12.1	0.637 ± 0.008	16 ± 3	-15.3 ± 0.3	-13.1 ± 0.5
CLY1_-115	*4.55*	*6*	*21.1 ± 0.1*	*25.4 ± 0.2*	*38*	*-5.5*	*-13.1*	*0.659 ± 0.018*	*10 ± 5*	*-16.1 ± 0.6*	*-15.5 ± 1.1*
CLY3_485490	4.88	7	21.6 ± 0.1	25.9 ± 0.2	6	-5.5	-11.8	0.661 ± 0.013	10 ± 4	-16.2 ± 0.4	-14.3 ± 0.8
CLY1_-80	*4.90*	*2*	–	–	*50*	*-5.9*	*-13.8*	*0.667 ± 0.038*	*8 ± 11*	*-16.7 ± 1.3*	*-16.6 ± 2.3*
CLY1_-15	*5.55*	*6*	*23.1 ± 0.1*	*27.4 ± 0.2*	*50*	*-6.5*	*-13.9*	*0.667 ± 0.008*	*8 ± 2*	*-17.3 ± 0.2*	*-16.7 ± 0.5*
CLY3_555560	5.88	4	25.5 ± 0.2	29.6 ± 0.4	8	-5.2	-12.4	0.600 ± 0.010	28 ± 3	-13.7 ± 0.4	-11.2 ± 0.6
CLY3_595600	6.28	5	24.7 ± 0.1	28.7 ± 0.3	6	-4.0	-12.1	0.564 ± 0.008	40 ± 3	-11.1 ± 0.4	-8.6 ± 0.6
WA-5 section											
WA5_80	0.80	4	6.9 ± 0.1	7.8 ± 0.1	3	-6.8	-12.3	0.640 ± 0.010	15 ± 3	-16.8 ± 0.3	-13.5 ± 0.6
WA5_95	0.95	4	–	–	5	-6.9	-12.2	0.620 ± 0.010	21 ± 3	-16.2 ± 0.3	-12.3 ± 0.6
WA5_110	1.10	5	6.7 ± 0.1	7.5 ± 0.1	4	-6.7	-12.4	0.607 ± 0.008	25 ± 3	-15.5 ± 0.3	-11.7 ± 0.5
WA5_126136m	1.31	4	12.8 ± 0.1	15.3 ± 0.2	5	-5.3	-13.4	0.613 ± 0.011	23 ± 4	-14.3 ± 0.4	-13.1 ± 0.7
WA5_122136p	*1.30*	*4*	*11.3 ± 0.1*	*13.1 ± 0.1*	*40*	*-6.2*	*-13.9*	*0.660 ± 0.012*	*10 ± 3*	*-16.8 ± 0.4*	*-16.3 ± 0.7*
WA5_155	1.55	5	–	–	3	-6.1	-14.5	0.645 ± 0.012	14 ± 4	-16.3 ± 0.4	-16.1 ± 0.8
WA5_175	1.75	6	14.5 ± 0.1	17.6 ± 0.2	3	-6.1	-15.0	0.657 ± 0.009	11 ± 2	-16.7 ± 0.3	-17.3 ± 0.5
WA5_195	1.95	3	16.9 ± 0.1	20.4 ± 0.2	3	-6.1	-15.1	0.612 ± 0.012	24 ± 4	-15.1 ± 0.4	-14.7 ± 0.8
WA5_225	2.25	3	18.7 ± 0.1	22.6 ± 0.2	3	-5.7	-13.9	0.658 ± 0.011	10 ± 3	-16.3 ± 0.4	-16.2 ± 0.7
WA5_265	2.65	3	–	–	11	-5.1	-14.1	0.609 ± 0.011	25 ± 4	-14.0 ± 0.4	-13.5 ± 0.7
WA5_285	2.85	7	27.1 ± 0.1	31.1 ± 0.2	12	-5.5	-14.3	0.611 ± 0.007	24 ± 2	-14.5 ± 0.3	-13.8 ± 0.5
WA5_290295	*2.93*	*10*	*26.2 ± 0.3*	*30.5 ± 0.6*	*60*	*-6.2*	*-15.4*	*0.678 ± 0.007*	*5 ± 2*	*-17.4 ± 0.2*	*-18.9 ± 0.4*
WA5_344	3.44	7	–	–	6	-4.0	-13.0	0.564 ± 0.015	40 ± 6	-11.1 ± 0.7	-9.5 ± 1.0
WA5_395400	3.98	8	27.3 ± 0.1	31.2 ± 0.2	6	-3.8	-11.9	0.568 ± 0.013	39 ± 5	-11.1 ± 0.6	-8.7 ± 0.9

Italicized samples denote macroscopic PCs (rhizoliths, root pore cements, burrow fills).

[*] Reported ^{14}C age uncertainties are 95% confidence intervals calculated using raw ^{14}C analytical errors (1σ) as input to OxCal 4.2 online calibration calculator (https://c14.arch.ox.ac.uk/oxcal/OxCal.html)

[**] Δ_{47} values reported in absolute reference frame (ARF) of Dennis et al. (2011). Δ_{47} standard error calculated as (sample Δ_{47} standard deviation)/$\sqrt{n}$. Minimum Δ_{47} st. dev. used = 0.19‰ (value for UW IsoLab carbonate standard C64).

[§] $T(\Delta_{47})$ calculated from sample average Δ_{47} values using T-Δ_{47} empirical calibration of Kelson et al. (2017).

[+] Soil CO_2 $\delta^{13}C$ value calculated using measured carbonate $\delta^{13}C_{VPDB}$, $T(\Delta_{47})$, and calcite-CO_2 ^{13}C fractionation equation of Romanek et al. (1992).

[‡] Water $\delta^{18}O$ value calculated using measured carbonate $\delta^{18}O_{VPDB}$, $T(\Delta_{47})$, and calcite-water ^{18}O fractionation equation of Coplen (2007). Uncertainties calculated using corresponding $T(\Delta_{47})$ S.E. values.

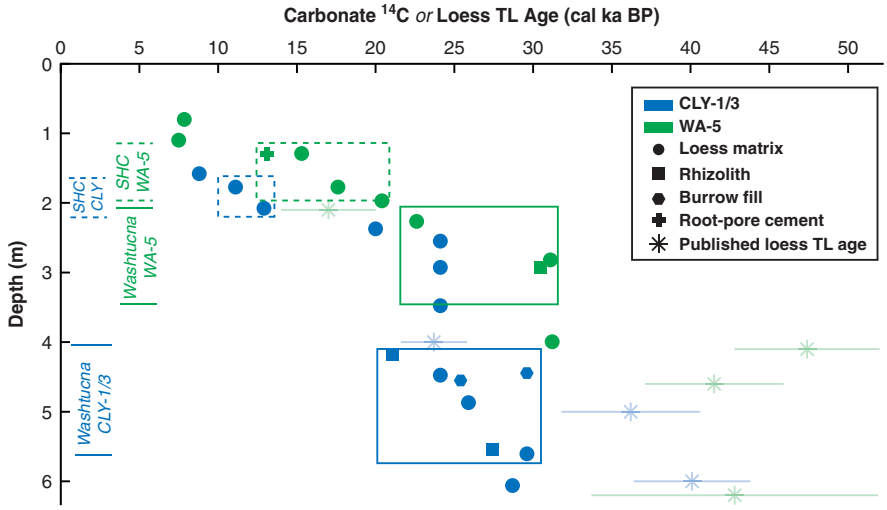

Figure 4. Carbonate ^{14}C records. Carbonate ^{14}C ages (this study) as a function of loess–paleosol column depth. Dashed boxes denote Sand Hills Coulee (SHC) paleosol at CLY-1/3 (blue) and WA-5 (green) study sections. Washtucna paleosol marked with solid boxes. Calibrated ^{14}C age uncertainties (95%) are smaller than symbol sizes (< ±1 ka). Published loess thermoluminescence (TL) ages from Berger and Busacca (1995) and Richardson et al. (1997) shown for reference. Published depths of loess TL samples reported for CLY-1/2 section in Richardson et al. (1997) have been converted to equivalent stratigraphic depths in CLY-1/3 section of this study. (For interpretation of the references to color in this figure legend, the reader is referred to the web version of this article.)

carbonate $\delta^{18}O$ values and temperature-sensitive, calcite-water oxygen isotope fractionation factors (Coplen, 2007). Soil CO_2 $\delta^{13}C$ values were determined from $T(\Delta_{47})$ and measured carbonate $\delta^{13}C$ values using the expression for $\Sigma_{calcite\text{-}CO_2}$ from Romanek et al. (1992) (Table 1).

We constrain loess–paleosol chronology using carbonate radiocarbon (^{14}C) dating. Radiocarbon activities of select carbonate samples were measured by DirectAMS (www.directams.net). Carbonate samples were digested under vacuum in phosphoric acid, and the liberated CO_2 was converted to graphite for analysis by accelerator mass spectrometry. Radiocarbon ages were calibrated using OxCal 4.2 (https://c14.arch.ox.ac.uk/oxcal/OxCal.html). All radiocarbon ages listed in Table 1 are reported in calibrated years before present (i.e., before 1950; abbreviated as cal ka BP). Given the potential for reservoir effects to bias soil carbonate ^{14}C ages older than they actually are (Yang et al., 1994) and the possibility that some component of analyzed loess matrix carbonate could be detrital and not formed in situ, reported radiocarbon ages should be interpreted as maximum values.

RESULTS

Carbonate ^{14}C

Radiocarbon ages for carbonate samples from CLY-1/3 and WA-5 vary systematically with depth (Fig. 4, Table 1). The ^{14}C analysis confirms that the shallowest, carbonate-bearing depths in each section contain Holocene-aged carbonate. Radiocarbon ages for carbonate sampled from the SHC paleosol at each section are consistent with a pre-Holocene, deglacial age of ~15–11 ka BP for the paleosol, as suggested by Sweeney et al. (2005). At CLY-1/3, an ~2.5-m-thick interval (modern depth 2.5–5 m) encompassing the Washtucna paleosol is characterized by uniform matrix carbonate ^{14}C ages of ~24 cal ka BP. Dated macroscopic PCs from throughout the Washtucna paleosol at CLY-1/3 range in ^{14}C age from ~30 to 21 cal ka BP. A similar age range (~31–20 cal ka BP) is observed across the Washtucna paleosol at WA-5. In both sections, loess matrix carbonates collected at depths below the Washtucna paleosol yield ^{14}C ages of ~31–28 cal ka BP. Carbonate ^{14}C ages thus confirm >10 ka pedogenic development (~31–20 cal ka BP) of the Washtucna paleosol leading up to and during the LGM (McDonald et al., 2012).

Carbonate $\delta^{18}O$ and $\delta^{13}C$

Measured loess matrix carbonate $\delta^{18}O$ and $\delta^{13}C$ values agree with published records at WA-5 (Takeuchi et al., 2009; Fig. 3). The $\delta^{13}C$ values generally increase with depth at both CLY-1/3 and WA-5, ranging from ~ −7‰ to −7.5‰ at shallow depths (<2 m) to ~ −4‰ within and near the last glacial–aged Washtucna paleosol. Carbonate $\delta^{18}O$ values also vary with depth. Maximum $\delta^{18}O$ values of ~ −10‰ to −12‰ are observed at the shallowest carbonate-bearing depths (0.8–1.5 m). Minimum $\delta^{18}O$ values (~ −13‰ to −15‰) characterize macroscopic PCs collected from within the Washtucna paleosol in both sections. At WA-5, similar minimum $\delta^{18}O$ values also characterize SHC interval carbonates, as observed in published loess matrix records (Takeuchi et al., 2009). In each section, $\delta^{18}O$ values of loess matrix carbonates are consistently 1–2‰ higher than those of macroscopic PCs at similar depths.

https://doi.org/10.1017/qua.2018.47 Published online by Cambridge University Press

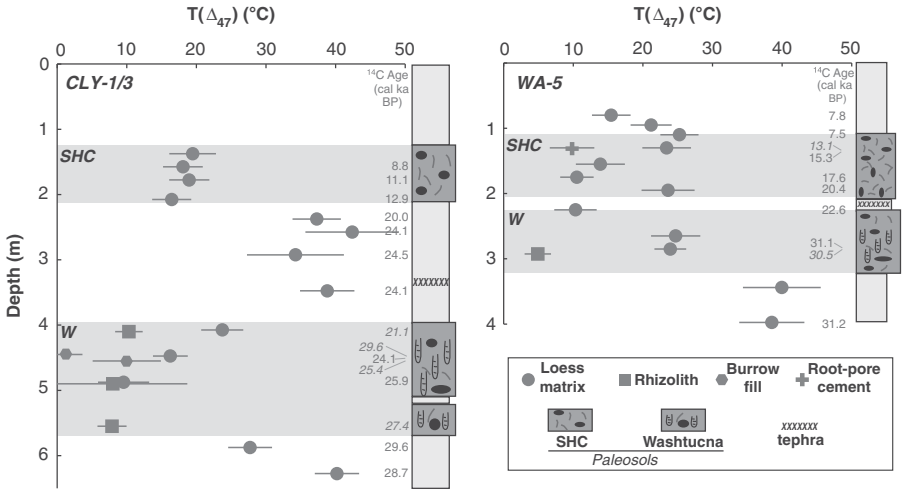

Figure 5. Carbonate T(Δ_{47}) records. Carbonate T(Δ_{47}) stratigraphic records for CLY-1/3 and WA-5 study sections. T(Δ_{47}) error bars show 1 standard error (Table 1). Carbonate ^{14}C ages for analyzed samples (Fig. 4) listed at depth of sampling (italics denotes macroscopic PC sample; see Table 1). Stratigraphic columns (Fig. 1B) shown for reference. SHC, Sand Hills Coulee paleosol; W, Washtucna paleosol.

Carbonate T(Δ_{47})

Similar to carbonate $\delta^{18}O$ and $\delta^{13}C$ trends, measured carbonate Δ_{47} and calculated T(Δ_{47}) values (Fig. 5, Table 1) vary with depth, carbonate type (loess matrix carbonate vs. macroscopic PC), and degree of pedogenesis (i.e., paleosol vs. poorly indurated loess). The total range of calculated T(Δ_{47}) values for samples from CLY-1/3 (1 ± 2°C to 42 ± 7°C [1 SE]) is similar to that of WA-5 (5 ± 2 to 40 ± 6°C) (Fig. 5, Table 1). In each section, macroscopic PCs collected from the Washtucna paleosol have the lowest T(Δ_{47}) values (1 ± 2°C to 10 ± 5°C). T(Δ_{47}) for Washtucna-paleosol loess matrix carbonates analyzed from each section overlap the warmer end of the T(Δ_{47}) range for macroscopic PCs but extend to warmer temperatures (10 ± 4°C to 25 ± 4°C). Although T(Δ_{47}) grossly varies with $CaCO_3$ wt% as a function of carbonate type (i.e., lower average T(Δ_{47}) for macroscopic PCs relative to loess matrix carbonates), among each carbonate type, T(Δ_{47}) values are not correlated with $CaCO_3$ wt% (Table 1; Online Supplementary Material, Fig. DR1).

The highest T(Δ_{47}) values (>30°C) observed in the CLY-1/3 and WA-5 study sections are associated with loess matrix samples from intervals exhibiting weak pedogenesis. At CLY-1/3, samples with T(Δ_{47}) > 30°C characterize intervals both above and below the defined Washtucna paleosol (modern depths 2.3–3.5 m and >6 m). At the more distal WA-5 site, where the SHC and Washtucna paleosols are separated by only a thin tephra layer (Fig. 1B), T(Δ_{47}) values >30°C are only observed for samples collected from depths below the Washtucna paleosol (>3.4 m depth). Samples with T(Δ_{47}) > 30°C are consistently characterized by the highest measured carbonate $\delta^{13}C$ and calculated T(Δ_{47}) standard error values ($\geq \pm 4$°C) in this sample data set (Fig. 5, Table 1). Conversely, carbonate $\delta^{18}O$ values do not covary with T(Δ_{47}) and instead are consistently low (< −11‰) for high-T(Δ_{47}) samples (Fig. 3, Table 1).

T(Δ_{47}) values are similar for Holocene-aged loess matrix carbonate from the shallowest Bk horizons in each section (18 ± 3°C to 19 ± 3°C at CLY-1/3, 15 ± 3°C to 25 ± 3°C at WA-5) and are within uncertainty (1 SE) of T(Δ_{47}) for samples from the SHC paleosol at CLY-1/3 (16 ± 3°C to 19 ± 3°C) and WA-5 (14 ± 4°C to 23 ± 4°C). However, root pore cements picked from the SHC paleosol at WA-5 (sample WA5_122136p; Fig. 2E and F) are offset to colder T(Δ_{47}) of 10 ± 3°C compared with loess matrix carbonate at the same depth (23 ± 4°C).

Water $\delta^{18}O_{VSMOW}$ values calculated using the equilibrium fractionation equation of Coplen (2007) (Fig. 6, Table 1) exhibit greater variability than corresponding carbonate $\delta^{18}O$ values (Fig. 3) and, in general, covary with carbonate T(Δ_{47}) (Fig. 7). Samples with T(Δ_{47}) > 30°C are characterized by the highest calculated water $\delta^{18}O_{VSMOW}$ values (−8‰ to −10‰). Washtucna paleosol macroscopic PCs with the lowest T(Δ_{47}) yield the lowest water $\delta^{18}O$ values, as low as −18.5‰ and −18.9‰ at CLY-1/3 and WA-5, respectively. Water $\delta^{18}O$ values calculated with the synthetic calcite–derived fractionation equation of Kim and O'Neil (1997) are ~1.7‰ higher than those calculated with the Coplen (2007) equation, but differences are near-uniformly shifted, such that water $\delta^{18}O$ variance, T(Δ_{47})-water $\delta^{18}O$ covariance, and time/depth trends do not change significantly (Online Supplementary Material, Table DR1).

Depth profiles of calculated soil CO_2 $\delta^{13}C$ (Fig. 6, Table 1) also track those of carbonate T(Δ_{47}) in study sections. Loess matrix samples with T(Δ_{47}) > 30°C have maximum soil CO_2 $\delta^{13}C_{VPDB}$ of −10.7‰ to −13.1‰ (Fig. 7). Minimum calculated soil CO_2 $\delta^{13}C$ values of −16.1‰ to −17.4‰ characterize the shallowest sampled intervals in each study section (Fig. 6). Similarly low soil CO_2 $\delta^{13}C$ values characterize macroscopic PCs with T(Δ_{47}) ≤ 10°C sampled within the Washtucna and SHC paleosols (Figs. 6 and 7). Washtucna paleosol loess matrix carbonates in each section yield intermediate soil CO_2 $\delta^{13}C$ estimates of −14‰ to −16.7‰.

https://doi.org/10.1017/qua.2018.47 Published online by Cambridge University Press

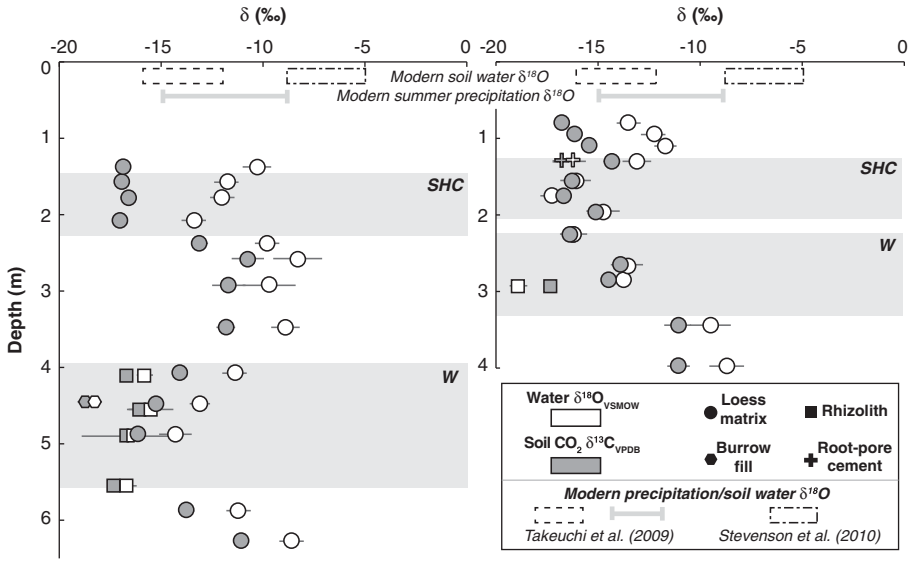

Figure 6. Water $\delta^{18}O$ and soil CO_2 $\delta^{13}C$ records. Calculated water $\delta^{18}O$ and soil CO_2 $\delta^{13}C$ for sample subsets analyzed for Δ_{47} (Fig. 5, Table 1). Error bars show 1 standard error propagated from T(Δ_{47}) standard error (Table 1). Note some samples have standard errors less than those of marker symbol sizes. Published modern soil water and summer precipitation $\delta^{18}O$ shown for reference: Stevenson et al. (2010) modern soil water $\delta^{18}O$ at Palouse sites with <400 mm MAP (sampled in June at 70 cm depth); Takeuchi et al. (2009) soil water and summer precipitation $\delta^{18}O$ at Pullman, WA (Fig. 1A) (soil water sampled December–June at depths of 25–90 cm; summer precipitation sampled April–September). SHC, Sand Hills Coulee paleosol; W, Washtucna paleosol.

DISCUSSION

Radiocarbon and isotopic results support the interpretation that the Palouse loess–paleosol carbonates examined here are pedogenic in origin and record meaningful paleoclimate information. That said, the variability in $\delta^{13}C$, $\delta^{18}O$, and T(Δ_{47}) values observed for penecontemporaneous Palouse carbonates suggests the need to consider potential impacts from PC type as well as variable depths and/or seasonal timings of PC formation. In the following subsections, we discuss how integration of radiocarbon geochronology and clumped isotope thermometry with conventional stable isotope study ($\delta^{13}C$, $\delta^{18}O$) of Palouse loess–paleosol carbonates aids paleoclimate reconstruction from these records.

Identifying a pedogenic origin for Palouse loess–paleosol carbonates

Paleoclimate interpretation of loess–paleosol proxy records requires that the studied carbonate is demonstrably pedogenic in origin or that pedogenic (secondary) components can be distinguished from any detrital (primary) carbonate present (e.g., Kemp, 2001; Zamanian et al., 2016). Carbonates preserved in $CaCO_3$-cemented paleosol intervals, including the macroscopic PCs (burrow fills, rhizoliths, and root-pore cements) analyzed for this study (Fig. 2), are demonstrably pedogenic (formed in situ) and thus suitable for paleoclimate interpretation. In contrast, submillimeter grain size prevents morphological identification of loess matrix carbonate origin, which can complicate paleoclimate reconstruction, given the potential for detrital carbonate components to remain unmodified in the loess matrix. Here, radiocarbon study of Palouse loess–paleosol carbonates provides needed insights.

Radiocarbon ages indicate a pedogenic origin for carbonates analyzed in this study, including loess matrix samples. If detrital carbonate was a significant component in studied intervals, carbonate radiocarbon ages would likely predate the age of loess deposition ("limestone dilution effect"; Williams and Polach, 1971; Chen and Polach, 1986). Conversely, PCs formed in situ should yield radiocarbon ages equal to or younger than the depositional ages of the loess that hosts them. Throughout the loess–paleosol sections studied here, carbonate radiocarbon ages are younger than or equal to published TL measures of depositional ages for the encompassing loess (Berger and Busacca, 1995; Richardson et al., 1997; Fig. 4), as expected for PCs. This suggests any detrital carbonate components incorporated into the loess when it was deposited were effectively overprinted by pedogenic processes during and/or following loess aggradation.

Additionally, minimum carbonate ^{14}C ages of ~8 cal ka BP at both CLY-1/3 and WA-5 suggest there has been minor (if any) incorporation of modern carbon into older PC via recrystallization and/or isotopic exchange after initial formation. Even where modern soil development occurs in close depth proximity to the SHC paleosol at WA-5 (Fig. 1B), ^{14}C ages for WA-5 SHC carbonates (20–13 cal ka BP) do not exhibit a bias toward younger ages that would reflect recrystallization or later-stage isotopic exchange. Palouse carbonate radiocarbon ages thus support interpretation of the loess soil carbonates analyzed for this study as pedogenic in origin and suitable for interpretation of last glacial period and Holocene soil conditions in the Palouse.

https://doi.org/10.1017/qua.2018.47 Published online by Cambridge University Press

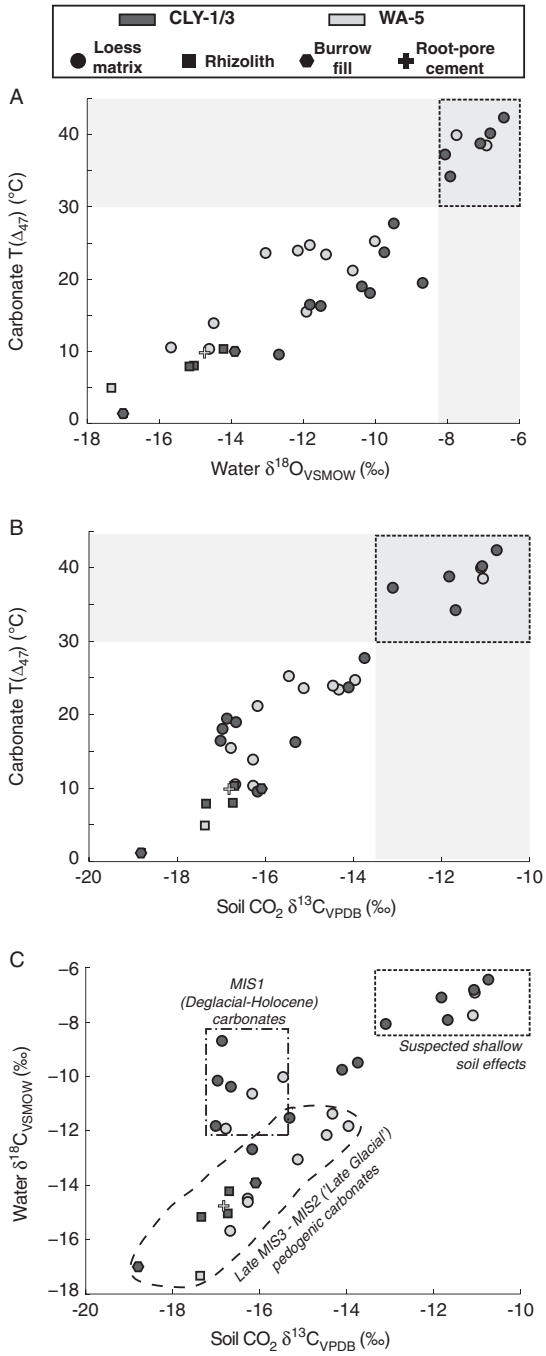

Figure 7. Summary of isotopic data. Note covariance of carbonate $T(\Delta_{47})$ with calculated water $\delta^{18}O$ (A) and soil CO_2 $\delta^{13}C$ (B). Gray swaths in A and B show $T(\Delta_{47})$ range (>30°C) and corresponding isotopic values interpreted to reflect conditions of shallow-soil formation (see text for discussion). (C) Calculated water $\delta^{18}O$ vs. soil CO_2 $\delta^{13}C$ with isotopic windows defined on basis of measured carbonate radiocarbon ages (Table 1) and interpretations from A and B. Modern soil water (December–June) and summer (April–September) precipitation $\delta^{18}O$ reported in Takeuchi et al. (2009) shown for reference (see Fig. 6). Note agreement of Marine Isotope Stage (MIS) 1 carbonate-derived and modern water $\delta^{18}O$ values.

Impact of carbonate type and shallow-soil effects on Palouse loess–paleosol proxy records

We integrate carbonate geochronology, $\delta^{13}C$, $\delta^{18}O$, and $T(\Delta_{47})$ data to evaluate the impacts of PC type and shallow-soil processes on our loess–paleosol proxy records. Stable and clumped isotope values vary by carbonate type, with macroscopic PCs characterized by $\delta^{13}C$, $\delta^{18}O$, and $T(\Delta_{47})$ values equal to or lower than those of loess matrix carbonates of similar age and/or stratigraphic position (Figs. 3 and 5, Table 1). Macroscopic PCs analyzed here come from well-developed paleosols characterized by stage III–IV carbonate morphologies (McDonald and Busacca, 1990), whereas loess matrix samples were collected from both paleosols and intervals of poorly indurated loess. Systematic variability in $\delta^{13}C$ and ^{14}C between macroscopic PCs and loess matrix carbonates was observed for loess–paleosol carbonates from the Nussloch sequence of SW Germany (Gocke et al., 2011). There, loess matrix carbonates with $\delta^{13}C$ values ~10‰ higher and ^{14}C ages >10 ka older than rhizolith carbonates at the same depth were identified to be detrital in origin (Gocke et al., 2011). However, carbonate radiocarbon ages obtained here rule out detrital effects to explain isotopic variability between macroscopic PCs and loess matrix carbonates at Palouse study sites. Instead, lower $\delta^{13}C$, $\delta^{18}O$, and $T(\Delta_{47})$ values for macroscopic PCs relative to penecontemporaneous in situ loess matrix carbonates suggest macroscopic PCs record more protracted (during the year) and sustained (occurring over multiple years/decades) periods of carbonate formation and more commonly formed at greater depth within the same (paleo)soil.

Carbonate encrustations of plant roots (rhizoliths) may form in direct association with active plant growth and respiration (e.g., Becze-Deák et al., 1997; Gocke et al., 2011). In the winter precipitation–dominated Palouse, peak growing season occurs as soils warm and dry out during the late spring to summer (Fig. 8), presumably making this the time of Palouse rhizolith formation. Association with root systems also promotes rhizolith development at depths of >0.5 m and in some cases >1 m below the (paleo)surface (e.g., Gocke et al., 2011). Accordingly, we interpret Palouse rhizoliths and other macroscopic PCs as proxies for warm-season, deeper (>0.5 m) soil conditions during the time of their formation.

In contrast, disseminated carbonate in the loess matrix can form via varied and potentially abiogenic mechanisms (Zamanian et al., 2016) making the seasonal timing/duration and depth of formation more difficult to ascertain. Further complicating interpretation of loess matrix proxies is the isotopic variability exhibited by Palouse loess matrix carbonates of similar ^{14}C age and/or stratigraphic position. Particularly notable are last glacial–aged (~31–24 cal ka BP) loess matrix samples from within and near the Washtucna paleosol that exhibit wide-ranging values of carbonate $T(\Delta_{47})$ (10–42°C), $\delta^{13}C_{VPDB}$ (–3.8‰ to –6‰), and calculated soil CO_2 $\delta^{13}C$ (–11.1‰ to –16.2‰) and water $\delta^{18}O$ (–8.6‰ to –14.3‰) (Figs. 3, 5, and 6, Table 1). We interpret this isotopic variability to reflect variable depths and seasonal

https://doi.org/10.1017/qua.2018.47 Published online by Cambridge University Press

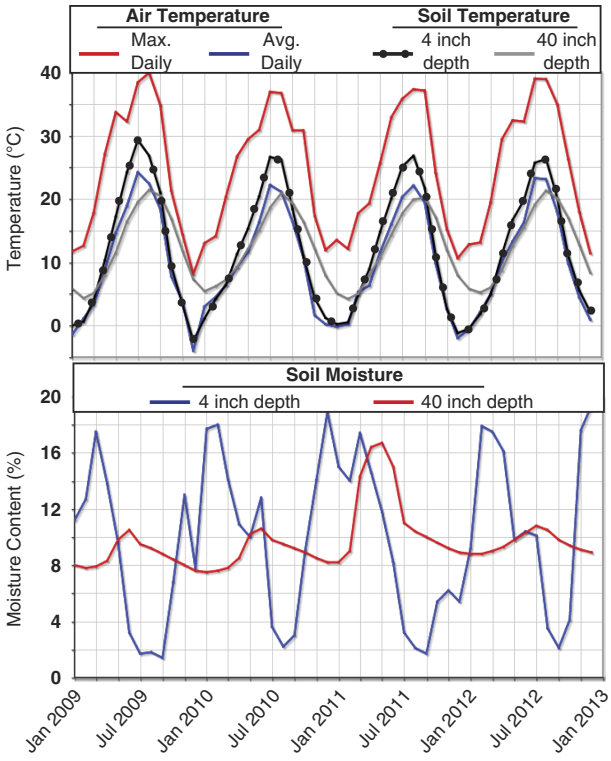

Figure 8. (color online) Modern soil-monitoring data for Lind, WA (see Fig. 1A for location). Note conditions that promote pedogenic carbonate formation (soil drying and warming) generally occur during the warm season (April–September). Data from http://www.wcc.nrcs.usda.gov (accessed July 28, 2015).

timings of loess matrix carbonate formation during the >10 ka development of the Washtucna paleosol.

Covariance of Palouse carbonate $T(\Delta_{47})$ with calculated soil CO_2 $\delta^{13}C$ and water $\delta^{18}O$ values (Fig. 7) can be used to constrain paleo-depths of formation in last glacial period soils of the Palouse. In modern soils, soil CO_2 $\delta^{13}C$, water $\delta^{18}O$, and temperature all exhibit a systematic decrease with depth during the warm season (e.g., Breecker et al., 2009; Quade et al., 2013), which we presume is the dominant season of PC formation for both the modern and last glacial period Palouse. Decreasing $\delta^{13}C$ (both carbonate and soil CO_2) with depth results from the increased component of low-$\delta^{13}C$, biologically respired CO_2 at greater depth in the soil. In arid to semiarid environments like the Palouse, this effect, along with probable kinetic isotope effects during calcite precipitation in the top several centimeters of soils, results in shallow-soil carbonate and CO_2 $\delta^{13}C$ values that are on the order of 5–10‰ higher than those at depth (>0.5 m) (Quade et al., 1989; Breecker et al., 2009). Similarly, as documented in the modern Palouse (Stevenson et al., 2010), soil water evaporation commonly results in shallow-soil waters having maximum $\delta^{18}O$ values. Soil temperature also decreases with depth during the summer, with shallow-soil (<0.25 m) temperatures up to 10–15°C higher than maximum daily air temperatures (Passey et al., 2010; Quade et al., 2013), which in the modern Palouse can reach ~40°C during the summer. In light of these trends, we interpret the association of maximum values of carbonate $T(\Delta_{47})$ (>30°C), $\delta^{13}C$ (> −5‰), and calculated soil CO_2 $\delta^{13}C$ (> −14‰) and water $\delta^{18}O$ (> −10‰) values observed for some glacial-aged loess matrix samples to reflect formation at shallow (<0.5 m) depths in the paleo-soil (Fig. 7).

Shallow-soil formation helps explain the distribution of loess matrix carbonates with uniform radiocarbon ages ~24 cal ka BP and high $T(\Delta_{47})$, $\delta^{13}C$, and water $\delta^{18}O$ values throughout the depth interval of ~2.5–4 m at CLY-1/3 (Figs. 4–6, Table 1). Immediately below, at ~4–5 m depth, loess matrix carbonates within the indurated Washtucna paleosol have equivalent radiocarbon ages but significantly lower $T(\Delta_{47})$ (10–25°C), $\delta^{13}C$ (< −5‰), and water $\delta^{18}O$ (< −11‰) values that are consistent with formation at depth (>0.5 m) in the paleosoil. We interpret the uniformity of radiocarbon ages across the 2.5–5 m interval to reflect a period of rapid loess accumulation at the CLY study site, dated here to ~24 cal ka BP, during which the active Bk horizon migrated upward and out of the indurated Washtucna interval, with only deep-penetrating roots continuing to reach the progressively buried paleosol (e.g., 21 cal ka BP rhizolith sample CLY1_-160; Table 1). Loess matrix carbonates with high $T(\Delta_{47})$, $\delta^{13}C$, and water $\delta^{18}O$ values at the 2.5–4 m depth are thus interpreted to reflect incipient PC formation that occurred within the uppermost portion of the aggrading loess soil column. Refined luminescence ages of loess deposition for the interval of 2.5–5 m depth are needed to fully evaluate this mechanism, but this plausibly explains why such a thick interval of uniform carbonate age is observed in the loess source proximal location of CLY-1/3, but not at the more distal WA-5 site, where loess accumulation rates were lower.

Potential influences from kinetic isotope effects and summer storm events on carbonate $T(\Delta_{47})$, $\delta^{13}C$, and $\delta^{18}O$

Warm $T(\Delta_{47})$ (34–42°C) for ~31–24 cal ka BP Palouse loess matrix samples are generally consistent with shallow depths of formation in the paleosoil column; however, shallow-soil (~10 cm depth) temperatures measured at the Lind, WA, Soil Climate Analysis Network site (Fig. 1A) rarely exceed 32°C, even when maximum daily temperatures are in excess of 40°C (Fig. 8). This calls into question whether apparent $T(\Delta_{47})$ values >32°C can be explained by warm-season carbonate formation in the shallow soil and suggests additional impacts from (1) kinetic isotope effects and/or (2) transient PC formation following summer storm events should also be considered.

Due to the slow rate of calcite precipitation at depth in (paleo)soils, PC should theoretically form in isotopic equilibrium with soil water and CO_2 (Cerling and Quade, 1993). However, disequilibrium and associated kinetic isotope effects (KIE) are known to impact carbonates precipitated in response to rapid CO_2 degassing. Such KIE have been shown to result in cave calcite $T(\Delta_{47})$, $\delta^{13}C$, and $\delta^{18}O$ values higher than those expected for equilibrium formation (Kluge and Affek, 2012) and have also been proposed to explain elevated

https://doi.org/10.1017/qua.2018.47 Published online by Cambridge University Press

$T(\Delta_{47})$, $\delta^{13}C$, and $\delta^{18}O$ values observed in modern high-elevation, hyperarid soils (Burgener et al., 2016). Consistent with KIE, Palouse samples with apparent $T(\Delta_{47}) > 32°C$ have the highest carbonate $\delta^{13}C$ values in the sample suite ($> -5‰$; Table 1), but this association is well explained by formation in the shallow (paleo)soil, as discussed. Moreover, carbonate $\delta^{18}O$ values for high-$T(\Delta_{47})$ Palouse samples are not anomalously high (Fig. 3), suggesting KIE did not measurably impact Palouse samples examined here. Accordingly, we interpret all analyzed Palouse carbonates to have formed in equilibrium.

To explain Palouse samples characterized by $T(\Delta_{47}) > 32°C$, we propose these loess matrix carbonates reflect brief and intermittent carbonate formation in the shallow paleosoil following individual warm-season precipitation events. This was shown to be a viable mechanism to explain $T(\Delta_{47})$ variability observed at shallow depths (≤40 cm) in modern soils in the western United States (Hough et al., 2014) and the Andes of South America (Burgener et al., 2016; Ringham et al., 2016). Such short-duration formation makes PC more sensitive to transient shallow-soil conditions, which in the case of summer rain events in the Palouse would commonly be associated with the maximum values of soil temperature and water $\delta^{18}O$ that appear to have been recorded by some glacial-aged Palouse loess matrix carbonates (Fig. 7).

Quantification of late glacial–Holocene climate change in the Palouse

Palouse loess matrix carbonates that record only shallow- and/or transient-soil conditions may provide limited or misleading insight into last glacial paleoenvironmental conditions. Accordingly, we base our last glacial climate reconstruction on samples interpreted to record integrated, deeper (>0.5 m depth) soil conditions, specifically those from the macroscopic PC–rich, well-indurated portion of the Washtucna paleosol (Fig. 9). Macroscopic PCs were not located during sampling of Holocene horizons at CLY-1/3 and WA-5, limiting reconstruction of Holocene paleoenvironmental conditions to loess matrix carbonates. Measured carbonate $\delta^{13}C$ and $\delta^{18}O$ and calculated water $\delta^{18}O$ values for Holocene loess matrix carbonates of this study are consistent with published records of regional Holocene carbonate $\delta^{13}C$ and $\delta^{18}O$ (Fig. 3) and modern soil water $\delta^{18}O$ (Takeuchi et al., 2009; Stevenson et al., 2010; Figs. 6 and 7). $T(\Delta_{47})$ values for Holocene carbonates analyzed here also overlap modern, shallow-soil (upper 1 m) temperatures in the Palouse that average ~20°C during the summer (Fig. 8). Together, these agreements suggest Holocene-aged loess matrix carbonates at CLY-1/3 and WA-5 are robust proxies for warm-season Holocene climate of the Palouse.

Presumably, loess matrix carbonates from the indurated portion of the Washtucna paleosol record comparable warm-season conditions for the late–last glacial period. Macroscopic PC development in last glacial Palouse soils was also likely promoted during the warm season, although lower $T(\Delta_{47})$, soil CO_2 $\delta^{13}C$, and water $\delta^{18}O$ values relative to loess

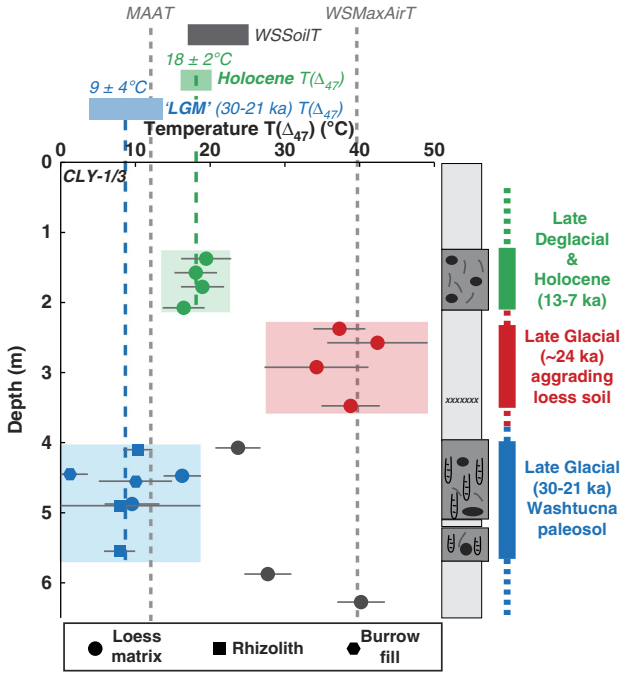

Figure 9. Paleoclimate interpretation of CLY-1/3 $T(\Delta_{47})$ record. Light-colored boxes show full $T(\Delta_{47})$ uncertainty and depth ranges for sample groupings discussed in the text. Average $T(\Delta_{47})$ for samples from the indurated portion of the Washtucna paleosol (blue; 9 ± 4°C) is significantly colder than that for the Holocene Bk interval (green, 18 ± 2°C). Note Holocene $T(\Delta_{47})$ overlaps modern regional warm-season soil temperatures (WSSoilT) (Fig. 8). The ~24 cal ka BP loess matrix samples with $T(\Delta_{47})$ >30°C (red) are interpreted to reflect shallow-soil effects in an aggrading soil column (see text for discussion). Regional mean annual air temperature (MAAT) and maximum warm season air temperature (WSMaxAirT) shown for reference. (For interpretation of the references to color in this figure legend, the reader is referred to the web version of this article.)

matrix carbonates of similar age and/or depth suggest that macroscopic PC formation was more distributed seasonally (i.e., not only during summer) and/or commonly occurred at greater depths in the paleosoil where soil temperature and water $\delta^{18}O$ more closely approximate mean annual rather than warm-season values (Breecker et al., 2009; Quade et al., 2013). We consider the potential effects from differences in the seasonal timing and/or depth of formation among Washtucna paleosol carbonate phases when quantifying last glacial–Holocene climate change in the Palouse.

Protracted development of the Washtucna paleosol throughout ~31–20 cal ka BP (Fig. 4) limits paleoclimate interpretation of its isotopic records to a multimillennial time scale. Accordingly, for interpretation of last glacial period paleoclimate, we group samples dated to the LGM proper (23–19 ka BP) with samples having slightly older, near-LGM ^{14}C ages of ~31–24 cal ka BP (grouping hereafter referred to as "late glacial"). Similarly, we group samples from the SHC paleosol with those dated to the Holocene, because there is no identifiable stratigraphic distinction between the modern Bk

https://doi.org/10.1017/qua.2018.47 Published online by Cambridge University Press

horizon and the late deglacial SHC paleosol, which is dated here to 15–11 cal ka BP (Fig. 4).

Identification of distinct late glacial and Holocene pedogenic intervals and quantification of magnitudes of late glacial–Holocene climate change is most reliably determined for the loess source-proximal CLY sequence. At CLY-1/3, average carbonate $\delta^{13}C_{VPDB}$ for Holocene samples (-7.3 ± 0.1‰ [$\pm$ 1 standard deviation]) is lower than the late glacial average (-6.0 ± 0.6‰); however, calculated late glacial soil CO_2 $\delta^{13}C_{VPDB}$ values (-16.7 ± 1.1‰) are within error of those for the Holocene (-16.9 ± 0.2‰; Fig. 8). Given the preponderance of evidence suggesting a more arid late glacial paleoclimate in the Palouse (Barnosky, 1985; Thompson et al., 1993; Whitlock and Bartlein, 1997; Blinnikov et al., 2001, 2002; Takeuchi et al., 2009; PMIP3 simulations), we presume such aridity changes are imprinted on Palouse proxy records despite the apparently unchanging soil CO_2 $\delta^{13}C$ values. Under conditions of lower atmospheric pCO_2 during the LGM (~190 ppm; Monnin et al., 2001) in a region of stable C_3-vegetation dominance like the Palouse (Blinnikov et al., 2001, 2002), no change in soil respiration rates would have resulted in lower LGM soil CO_2 $\delta^{13}C_{VPDB}$ values (i.e., less high-$\delta^{13}C$ atmospheric input). Therefore, similar soil CO_2 $\delta^{13}C$ for the late glacial and Holocene intervals suggests that influence on soil CO_2 $\delta^{13}C$ from lower pCO_2 during the LGM was offset by either (1) lower LGM soil respiration rates as a result of increased regional aridity, (2) higher LGM organic matter $\delta^{13}C$ values due to higher aridity/lower pCO_2 (see Schubert and Jahren, 2015; Breecker, 2017), or (3) both LGM soil respiration rates were lower and organic matter $\delta^{13}C$ values were higher. In any case, we interpret the stability of calculated soil CO_2 $\delta^{13}C$ values from the late glacial into the Holocene as a record of the approximate balance between atmospheric and vegetative controls on Palouse soil CO_2 $\delta^{13}C$ through time.

The $T(\Delta_{47})$ record at CLY also enables us to quantify the magnitude of regional cooling during the late glacial. The difference in average $T(\Delta_{47})$ for Washtucna paleosol rhizolith and burrow-fill carbonates (7 ± 4°C; $n = 5$) and for loess matrix carbonates (13 ± 5°C; $n = 2$) at CLY-1/3 is not statistically significant (Student's *t*-test *P* value = 0.13). As a result, we group together Washtucna macroscopic PCs and loess matrix carbonates when quantifying paleoenvironmental conditions of the late glacial Palouse (Fig. 9). The resulting average late glacial $T(\Delta_{47})$ of 9 ± 4°C is significantly lower than average $T(\Delta_{47})$ for SHC Holocene carbonates of 18 ± 1°C (*P* value = 0.003; Fig. 9) as well as the observed range for modern warm-season soil temperatures in the Palouse (~18–22°C; Fig. 8). Interpreted simply, this $T(\Delta_{47})$ difference indicates regional warm-season soil and surface temperatures leading up to and during the LGM were 9 ± 5°C colder than modern which agrees with simulated magnitudes of LGM–Holocene warm-season (June-September) temperature change across the Palouse region (~5–15°C; PMIP3 simulations; Bartlein et al., 2011). This magnitude of temperature change could be an overestimate, given the typically higher temperatures for loess matrix carbonates compared with penecontemporaneous macroscopic PCs. Using only equivalent loess matrix phases from late glacial and Holocene intervals at CLY-1/3 yields a conservative estimate of late glacial–Holocene warming of ~5°C. PMIP3 outputs show that magnitudes of LGM–Holocene warm-season temperature change in the Palouse were similar to regional MAT change. As a result, we interpret the calculated Holocene–late glacial T (Δ_{47}) difference of 9 ± 5°C also as the magnitude of late glacial mean annual cooling across the Palouse region, a magnitude that matches that of recent proxy-model synthesis (4-12°C; Annan and Hargreaves, 2013).

Calculated soil water $\delta^{18}O$ values also reflect a measurably colder late glacial Palouse region. The observed shift in average soil water $\delta^{18}O_{VSMOW}$ values from the late glacial (-16 ± 2‰) to the Holocene (-11 ± 1‰; Fig. 7) suggests late glacial precipitation/soil water $\delta^{18}O$ values were 2–8‰ lower than those of the Holocene. This magnitude of change is generally consistent with GCM-simulated changes in precipitation $\delta^{18}O$ across the most recent glacial–interglacial transition, which have been interpreted to have resulted from colder mean annual temperatures during the LGM (Jouzel et al., 1994; Jasechko et al., 2015).

Paleoclimate interpretation of the WA-5 record is less clear than that of CLY-1/3, because the lack of a single-age paleosoil column at WA-5 makes it difficult to assess the depths of WA-5 carbonate sample formation in the paleosoil and the associated influences on isotopic values. That said, overall $T(\Delta_{47})$, $\delta^{13}C$, and $\delta^{18}O$ trends and variability for the WA-5 record are consistent with those observed at CLY-1/3 (Fig. 7). At WA-5, Washtucna paleosol $T(\Delta_{47})$ ranges from 5 ± 2°C for a 30.5 cal ka BP rhizolith up to 40 ± 6°C for loess matrix carbonate bracketed by 31.1 and 31.2 cal ka BP radiocarbon ages (Fig. 5). Similar to our interpretation of the CLY-1/3 record (Fig. 9), we interpret the ~35°C spread in carbonate $T(\Delta_{47})$ across the Washtucna paleosol at WA-5 to reflect variable seasonal timings and influences from shallow-soil processes during the ~10 ka development of the late glacial Washtucna paleosol. This $T(\Delta_{47})$ variability limits our ability to quantify late glacial–Holocene temperature change from the WA-5 record; however, like CLY-1/3, minimum $T(\Delta_{47})$ at WA-5 (5 ± 2°C) is preserved in the Washtucna paleosol and is significantly colder than both modern warm-season soil temperatures (Fig. 8) and the range of $T(\Delta_{47})$ values measured for Holocene carbonates (15–25°C) in the WA-5 section. Together, CLY-1/3 and WA-5 carbonate $T(\Delta_{47})$ records indicate a measurably colder late glacial climate across the Palouse region with a magnitude of warm-season and mean annual temperature change of 9 ± 5°C that is in agreement with published LGM model simulations (PMIP3) and proxy-model syntheses (Bartlein et al., 2011; Annan and Hargreaves, 2013).

CONCLUSIONS

Integrated $T(\Delta_{47})$ and radiocarbon study of Palouse loess–paleosol carbonates offers new insight into quantitative

https://doi.org/10.1017/qua.2018.47 Published online by Cambridge University Press

magnitudes of regional surface/soil temperature, soil CO_2 $\delta^{13}C$, and meteoric water $\delta^{18}O$ change across the most recent glacial–interglacial transition in a region proximal to the Cordilleran Ice Sheet. Our work helps to discern which carbonate-bearing intervals in Palouse loess–paleosols serve as robust paleoclimate archives. Carbonate ^{14}C ages suggest all loess–paleosol carbonates analyzed for this study formed in situ in Palouse loess (paleo)soils, including loess matrix carbonates. Association of high $T(\Delta_{47})$, soil CO_2 $\delta^{13}C$ values, and calculated meteoric water $\delta^{18}O$ values for loess matrix carbonates dating to the late glacial period (~31–20 cal ka BP) points to the influence that shallow-soil and transient PC formation processes can imprint on these proxy records. Accounting for these effects, Palouse loess–paleosol $T(\Delta_{47})$ and water $\delta^{18}O$ records vary coherently with paleoclimate state. Average $T(\Delta_{47})$ for carbonates from the late glacial Washtucna paleosol (9 ± 4°C) in comparison to Holocene $T(\Delta_{47})$ (18 ± 2°C) suggests the regional paleoclimate of the Palouse leading up to and during the LGM was 9 ± 5°C cooler than that of the Holocene. Changes in calculated soil water $\delta^{18}O$ values from the late glacial (-16 ± 2‰) to the Holocene (-11 ± 1‰) also reflect impacts of a cooler last glacial paleoclimate on regional precipitation $\delta^{18}O$. These magnitudes of last glacial–Holocene change in the Palouse agree with published LGM paleoclimate simulations and ensemble studies and aid understanding of the impact that extensive and thick (>1 km) North American continental ice sheets had for the late Pleistocene paleoclimate of the PNW. Our work supports previous findings that clumped isotope thermometry of loess–paleosols can provide valuable, quantitative paleoenvironmental information (Eagle et al., 2013) and highlights the importance of considering potential influences from PC type, shallow-soil processes, and seasonal timing of carbonate formation when reconstructing paleoclimate from these proxy archives.

SUPPLEMENTARY MATERIAL

To view supplementary material for this article, please visit https://doi.org/10.1017/qua.2018.47

ACKNOWLEDGMENTS

This work was supported by grants awarded from the M.J. Murdock College Research Program for Natural Sciences (grant #2014273 to A.R. Lechler), the U.S. National Science Foundation (EAR-125206 to K.W. Huntington), and the Quaternary Research Center at the University of Washington, in addition to student research support provided to A.R. Lechler by the Pacific Lutheran University Division of Natural Sciences. We thank Landon Burgener, Kelly Egaas, Dave Ruppert, Kyle Gosnell, Justin Johnsen, and Isabellah von Trapp for assistance with field sampling and sample preparation, and Kyle Samek for assistance with laboratory analysis. Two anonymous reviewers, associate editor Matthew Lachniet, and senior editor Nicholas Lancaster are thanked for reviews that enhanced the presentation and clarity of this article.

REFERENCES

Affek, H.P., 2012. Clumped isotope paleothermometry: principles, applications, and challenges. In: *Reconstructing Earth's Deep-Time Climate—The State of the Art in 2012*, Paleontological Society Papers, Vol. 18. Paleontological Society, Boulder, CO, pp.101–114.

Annan, J.D., Hargreaves, J.C., 2013. A new global reconstruction of temperature changes at the Last Glacial Maximum. *Climate of the Past* 9, 367–376.

Annan, J.D., Hargreaves, J.C., 2015. A perspective on model-data surface temperature comparison at the Last Glacial Maximum. *Quaternary Science Reviews* 107, 1–10.

Bader, N.E., Spencer, P.K., Bailey, A.S., Gastineau, K.M., Tinkler, E.R., Pluhar, C.J., Bjornstad, B.N., 2016. A loess record of pre-Late Wisconsin glacial outburst flooding, Pleistocene paleoenvironment, and Irvingtonian fauna from the Rulo site, southeastern Washington, USA. *Palaeogeography, Palaeoclimatology, Palaeoecology* 462, 57–69.

Baker, V.R., 2009. The Channeled Scabland: a retrospective. *Annual Review of Earth and Planetary Sciences* 37, 393–411.

Baker, V.R., Bjornstad, B.N., Busacca, A.J., Fecht, K.R., Kiver, E.P., Moody, U.L., Rigby, J.G., Stradling, D.F., Tallman, A.M., 1991. Quaternary geology of the Columbia Plateau. In, *Quaternary Nonglacial Geology: Conterminous US*. Geology of North America Vol. 2. Geological Society of America, Boulder, CO, pp. 215–250.

Baker, V.R., Bjornstad, B.N., Gaylord, D.R., Smith, G.A., Meyer, S.E., Alho, P., Breckenridge, R.M., Sweeney, M.R., Zreda, M., 2016. Pleistocene megaflood landscapes of the Channeled Scabland. In: Lewis, R.S., Schmidt, K.L. (Eds.), *Exploring the Geology of the Inland Northwest*. Geological Society of America Field Guide 41, Geological Society of America, Boulder, CO, pp. 1–73.

Baker, V.R., Bunker, R.C., 1985. Cataclysmic late Pleistocene flooding from glacial Lake Missoula: a review. *Quaternary Science Reviews* 4, 1–41.

Barnosky, C.W., 1985. Late Quaternary vegetation in the southwestern Columbia basin, Washington. *Quaternary Research* 23, 109–122.

Bartlein, P.J., Anderson, K.H., Anderson, P.M., Edwards, M.E., Mock, C.J., Thompson, R.S., Webb, R.S., Webb, T., III, Whitlock, C., 1998. Paleoclimate simulations for North America over the past 21,000 years: features of the simulated climate and comparisons with paleoenvironmental data. *Quaternary Science Reviews* 17, 549–585.

Bartlein, P.J., Harrison, S.P., Brewer, S., Connor, S., Davis, B.A.S., Gajewski, K., Guiot, J., et al., 2011. Pollen-based continental climate reconstructions at 6 and 21 ka: a global synthesis. *Climate Dynamics* 37, 775–802.

Becze-Deák, J., Langohr, R., Verrecchia, E.P., 1997. Small scale secondary $CaCO_3$ accumulations in selected sections of the European loess belt. Morphological forms and potential for paleoenvironmental reconstruction. *Geoderma* 76, 221–252.

Berger, G.W., Busacca, A.J., 1995. Thermoluminescence dating of late Pleistocene loess and tephra from eastern Washington and southern Oregon and implications for the eruptive history of Mount St. Helens. *Journal of Geophysical Research: Solid Earth (1978–2012)* 100(B11), 22361–22374.

Blinnikov, M., Busacca, A., Whitlock, C., 2001. A new 100,000-year phytolith record from the Columbia Basin, Washington, USA. In Meunier, J.D., Colin, F., *Phytoliths: Applications in Earth Sciences and Human History*. Balkema, Lisse, Netherlands, pp. 27–55.

Blinnikov, M., Busacca, A., Whitlock, C., 2002. Reconstruction of the late Pleistocene grassland of the Columbia basin, Washington, USA, based on phytolith records in loess. *Palaeogeography, Palaeoclimatology, Palaeoecology* 177, 77–101.

Boling, M., Frazier, B., Busacca, A.J., 1998. *General Soil Map, Washington*. Department of Crop and Soil Sciences, Washington State University, Pullman.

Booth, D.B., Troost, K.G., Clague, J.J., Waitt, R.B., 2003. The Cordilleran ice sheet. *Developments in Quaternary Sciences* 1, 17–43.

Braconnot, P., Harrison, S.P., Kageyama, M., Bartlein, P.J., Masson-Delmotte, V., Abe-Ouchi, A., Otto-Bliesner, B., Zhao, Y., 2012. Evaluation of climate models using palaeoclimatic data. *Nature Climate Change* 2, 417–424.

Breecker, D.O., 2017. Atmospheric pCO_2 control on speleothem stable carbon isotope compositions. *Earth and Planetary Science Letters* 458, 58–68.

Breecker, D.O., Sharp, Z.D., McFadden, L.D., 2009. Seasonal bias in the formation and stable isotopic composition of pedogenic carbonate in modern soils from central New Mexico, USA. *Geological Society of America Bulletin* 121, 630–640.

Bretz, J.H., 1923. The channeled scablands of the Columbia Plateau. *Journal of Geology* 31, 617–649.

Bretz, J.H., 1969. The Lake Missoula floods and the channeled scabland. *Journal of Geology* 77, 505–543.

Bromwich, D.H., Toracinta, E.R., Wei, H., Oglesby, R.J., Fastook, J.L., Hughes, T.J., 2004. Polar MM5 simulations of the winter climate of the Laurentide Ice Sheet at the LGM. *Journal of Climate* 17, 3415–3433.

Bromwich, D.H., Toracinta, E.R., Oglesby, R.J., Fastook, J.L., Hughes, T.J., 2005. LGM summer climate on the southern margin of the Laurentide Ice Sheet: wet or dry? *Journal of Climate* 18, 3317–3338.

Burgener, L., Huntington, K.W., Hoke, G.D., Schauer, A., Ringham, M.C., Latorre, C., Díaz, F.P., 2016. Variations in soil carbonate formation and seasonal bias over 4 km of relief in the western Andes (30 S) revealed by clumped isotope thermometry. *Earth and Planetary Science Letters* 441, 188–199.

Busacca, A. J., 1989. Long Quaternary record in eastern Washington, USA, interpreted from multiple buried paleosols in loess. *Geoderma* 45, 105–122.

Busacca, A.J., McDonald, E.V., 1994. Regional sedimentation of late Quaternary loess on the Columbia Plateau: sediment source areas and loess distribution patterns. *Washington Division of Geology and Earth Resources Bulletin* 80, 181–190.

Cerling, T.E., Quade, J., 1993. Stable carbon and oxygen isotopes in soil carbonates. In: Swart, P.K., Lohmann, K.C., McKenzie, J., Savin, S. (Eds.), *Climate Change in Continental Isotopic Records*, American Geophysical Union, Washington, DC, pp. 217–231.

Chen, Y., Polach, H., 1986. Validity of ^{14}C ages of carbonates in sediments. *Radiocarbon* 28, 464–472.

Clague, J.J., 2009. Cordilleran ice sheet. In, *Encyclopedia of Paleoclimatology and Ancient Environments*. Springer, Dordrecht, Netherlands, pp. 206–211.

Clague, J.J., Barendregt, R., Enkin, R.J., Foit, F.F., 2003. Paleomagnetic and tephra evidence for tens of Missoula floods in southern Washington. *Geology* 31, 247–250.

Clynne, M. A., Calvert, A.T., Wolfe, E.W., Evarts, R.C., Fleck, R.J., Lanphere, M.A., 2008. The Pleistocene eruptive history of Mount St. Helens, Washington, from 300,000 to 12,800 years before present. In: Sherrod, D.R., Scott, W.E., Stauffer, P.H. (Eds.), *A Volcano Rekindled; the Renewed Eruption of Mount St Helens, 2004–2006*. U.S. Geological Survey Professional Paper 1750, USGS Information Services, Denver, CO, pp. 647–702.

COHMAP Members. 1988. Climatic changes of the last 18,000 years: observations and model simulations. *Science* 241, 1043–1052.

Coplen, T.B., 2007. Calibration of the calcite–water oxygen-isotope geothermometer at Devils Hole, Nevada, a natural laboratory. *Geochimica et Cosmochimica Acta* 71, 3948–3957.

Dennis, K.J., Affek, H.P., Passey, B.H., Schrag, D.P., Eiler, J.M., 2011. Defining an absolute reference frame for "clumped" isotope studies of CO_2. *Geochimica et Cosmochimica Acta* 75, 7117–7131.

Eagle, R.A., Risi, C., Mitchell, J.L., Eiler, J.M., Seibt, U., Neelin, J. D., Gaojun, L., Tripati, A.K., 2013. High regional climate sensitivity over continental China constrained by glacial-recent changes in temperature and the hydrological cycle. *Proceedings of the National Academy of Sciences USA* 110, 8813–8818.

Eiler, J.M., 2007. "Clumped-isotope" geochemistry—the study of naturally-occurring, multiply-substituted isotopologues. *Earth and Planetary Science Letters* 262, 309–327.

Eiler, J.M., 2011. Paleoclimate reconstruction using carbonate clumped isotope thermometry. *Quaternary Science Reviews* 30, 3575–3588.

Gaylord, D.R., Busacca, A.J., Sweeney, M.R., 2003. The Palouse loess and the Channeled Scabland: a paired Ice-Age geologic system. In: Easterbrook, D.J. (Ed.), *Quaternary Geology of the United States*. INQUA 2003 Field Guide Volume, Desert Research Institute, Reno, NV, pp. 123–134.

Ghosh, P., Adkins, J., Affek, H., Balta, B., Guo, W., Schauble, E.A., Schrag, D., Eiler, J.M., 2006. 13 C–18 O bonds in carbonate minerals: a new kind of paleothermometer. *Geochimica et Cosmochimica Acta* 70, 1439–1456.

Gocke, M., Pustovoytov, K., Kühn, P., Wiesenberg, G.L.B., Löscher, M., Kuzyakov, Y., 2011. Carbonate rhizoliths in loess and their implications for paleoenvironmental reconstruction revealed by isotopic composition: $\delta^{13}C$, ^{14}C. *Chemical Geology* 283, 251–260.

Hanson, M.A., Lian, O.B., Clague, J.J., 2012. The sequence and timing of large late Pleistocene floods from glacial Lake Missoula. *Quaternary Science Reviews* 31, 67–81.

Hargreaves, J.C., Paul, A., Ohgaito, R., Abe-Ouchi, A., Annan, J.D., 2011. Are paleoclimate model ensembles consistent with the MARGO data synthesis? *Climate of the Past* 7, 917–933.

Harrison, S.P., Bartlein, P.J., Izumi, K., Li, G., Annan, J., Hargreaves, J., Braconnot, P., Kageyama, M., 2015. Evaluation of CMIP5 palaeo-simulations to improve climate projections. *Nature Climate Change* 5, 735–743.

He, B., Olack, G.A., Colman, A.S., 2012. Pressure baseline correction and high-precision CO_2 clumped-isotope (Δ_{47}) measurements in bellows and micro-volume modes. *Rapid Communications in Mass Spectrometry* 26, 2837–2853.

Hough, B.G., Fan, M., Passey, B.H., 2014. Calibration of the clumped isotope geothermometer in soil carbonate in Wyoming and Nebraska, USA: implications for paleoelevation and paleoclimate reconstruction. *Earth and Planetary Science Letters* 391, 110–120.

Huntington, K.W., Eiler, J.M., Affek, H.P., Guo, W., Bonifacie, M., Yeung, L.Y., Thiagarajan, N., *et al.*, 2009. Methods and limitations of "clumped" CO_2 isotope ($\Delta 47$) analysis by gas-source isotope ratio mass spectrometry. *Journal of Mass Spectrometry* 44, 1318–1329.

https://doi.org/10.1017/qua.2018.47 Published online by Cambridge University Press

Huntington, K.W., Lechler, A.R., 2015. Carbonate clumped isotope thermometry in continental tectonics. *Tectonophysics* 647, 1–20.

Jasechko, S., Lechler, A., Pausata, F.S.R., Fawcett, P.J., Gleeson, T., Cendón, D.I., Galewsky, J., et al., 2015. Glacial–interglacial shifts in global and regional precipitation $\delta^{18}O$. *Climate of the Past Discussions* 11, 831–872.

Jouzel, J., Koster, R.D., Suozzo, R.J., Russell, G.L., 1994. Stable water isotope behavior during the last glacial maximum: a general circulation model analysis. *Journal of Geophysical Research: Atmospheres (1984–2012)* 99(D12), 25791–25801.

Kelson, J.R., Huntington, K.W., Schauer, A.J., Saenger, C., Lechler, A.R., 2017. Toward a universal carbonate clumped isotope calibration: diverse synthesis and preparatory methods suggest a single temperature relationship. *Geochimica et Cosmochimica Acta* 197, 104–131.

Kemp, R.A., 2001. Pedogenic modification of loess: significance for palaeoclimatic reconstructions. *Earth-Science Reviews* 54, 145–156.

Kim, S.T., O'Neil, J.R., 1997. Equilibrium and nonequilibrium oxygen isotope effects in synthetic carbonates. *Geochimica et Cosmochimica Acta* 61, 3461–3475.

Kluge, T., Affek, H.P., 2012. Quantifying kinetic fractionation in Bunker Cave speleothems using Δ47. *Quaternary Science Reviews* 49, 82–94.

Kutzbach, J.E., Wright, H.E., 1985. Simulation of the climate of 18,000 years BP: results for the North American/North Atlantic/European sector and comparison with the geologic record of North America. *Quaternary Science Reviews* 4, 147–187.

MARGO Project Members. 2009. Constraints on the magnitude and patterns of ocean cooling at the Last Glacial Maximum. *Nature Geoscience* 2, 127–132.

McDonald, E.V., Busacca, A.J., 1990. Interaction between aggrading geomorphic surfaces and the formation of a Late Pleistocene paleosol in the Palouse loess of eastern Washington state. *Geomorphology* 3, 449–469.

McDonald, E.V., Busacca, A.J., 1992. Late Quaternary stratigraphy of loess in the Channeled Scabland and Palouse regions of Washington State. *Quaternary Research* 38, 141–156.

McDonald, E.V., Sweeney, M.R., Busacca, A.J., 2012. Glacial outburst floods and loess sedimentation documented during Oxygen Isotope Stage 4 on the Columbia Plateau, Washington State. *Quaternary Science Reviews* 45, 18–30.

Mix, A.C., Bard, E., Schneider, R., 2001. Environmental processes of the ice age: land, oceans, glaciers (EPILOG). *Quaternary Science Reviews* 20, 627–657.

Monnin, E., Indermühle, A., Daellenbach, A., Flueckiger, J., Stauffer, B., Stocker, T.F., Raynaud, D., Barnola, J.-M., 2001. Atmospheric CO2 concentrations over the Last Glacial Termination. *Science* 291, 112–114.

O'Connor, J.E., Baker, V.R., 1992. Magnitudes and implications of peak discharges from glacial Lake Missoula. *Geological Society of America Bulletin* 104, 267–279.

O'Geen, A.T., Busacca, A.J., 2001. Faunal burrows as indicators of paleo-vegetation in eastern Washington, USA. *Palaeogeography, Palaeoclimatology, Palaeoecology* 169, 23–37.

Otto-Bliesner, B.L., Schneider, R., Brady, E.C., Kucera, M., Abe-Ouchi, A., Bard, E., Braconnot, P., *et al.*, 2009. A comparison of PMIP2 model simulations and the MARGO proxy reconstruction for tropical sea surface temperatures at last glacial maximum. *Climate Dynamics* 32, 799–815.

Passey, B.H., 2012. Reconstructing terrestrial environments using stable isotopes in fossil teeth and paleosol carbonates. In: *Reconstructing Earth's Deep-Time Climate—the State of the Art in 2012*, Paleontological Society Papers, Vol. 18. Paleontological Society, Boulder, CO, pp. 167–193.

Passey, B.H., Levin, N.E., Cerling, T.E., Brown, F.H., Eiler, J.M., 2010. High-temperature environments of human evolution in East Africa based on bond ordering in paleosol carbonates. *Proceedings of the National Academy of Sciences USA* 107, 11245–11249.

Pluhar, C.J., Bjornstad, B.N., Reidel, S.P., Coe, R.S., Nelson, P.B., 2006. Magnetostratigraphic evidence from the Cold Creek bar for onset of ice-age cataclysmic floods in eastern Washington during the Early Pleistocene. *Quaternary Research* 65, 123–135.

Quade, J., Cerling, T.E., Bowman, J.R., 1989. Systematic variations in the carbon and oxygen isotopic composition of pedogenic carbonate along elevation transects in the southern Great Basin, United States. *Geological Society of America Bulletin* 101, 464–475.

Quade, J., Eiler, J., Daëron, M., Achyuthan, H., 2013. The clumped isotope geothermometer in soil and paleosol carbonate. *Geochimica et Cosmochimica Acta* 105, 92–107.

Richardson, C.A., McDonald, E.V., Busacca, A.J., 1997. Luminescence dating of loess from the northwest United States. *Quaternary Science Reviews* 16, 403–415.

Ringham, M.C., Hoke, G.D., Huntington, K.W., Aranibar, J.N., 2016. Influence of vegetation type and site-to-site variability on soil carbonate clumped isotope records, Andean piedmont of Central Argentina (32–34 S). *Earth and Planetary Science Letters* 440, 1–11.

Romanek, C.S., Grossman, E.L., Morse, J.W., 1992. Carbon isotopic fractionation in synthetic aragonite and calcite: effects of temperature and precipitation rate. *Geochimica et Cosmochimica Acta* 56, 419–430.

Ross, S.M., 2003. Peirce's criterion for the elimination of suspect experimental data. *Journal of Engineering Technology* 20, 38–41.

Schauble, E.A., Ghosh, P., Eiler, J.M., 2006. Preferential formation of 13 C–18 O bonds in carbonate minerals, estimated using first-principles lattice dynamics. *Geochimica et Cosmochimica Acta* 70, 2510–2529.

Schauer, A.J., Kelson, J., Saenger, C., Huntington, K.W., 2016. Choice of ^{17}O correction affects clumped isotope (Δ_{47}) values of CO_2 measured with mass spectrometry. *Rapid Communications in Mass Spectrometry* 30, 2607–2616.

Schmittner, A., Urban, N.M., Shakun, J.D., Mahowald, N.M., Clark, P.U., Bartlein, P.J., Mix, A.C., Rosell-Melé, A., 2011. Climate sensitivity estimated from temperature reconstructions of the Last Glacial Maximum. *Science* 334, 1385–1388.

Schubert, B.A., Jahren, A.H., 2015. Global increase in plant carbon isotope fractionation following the Last Glacial Maximum caused by increase in atmospheric pCO_2. *Geology* 43, 435–438.

Stevenson, B.A., Kelly, E.F., McDonald, E.V., Busacca, A.J., 2005. The stable carbon isotope composition of soil organic carbon and pedogenic carbonates along a bioclimatic gradient in the Palouse region, Washington State, USA. *Geoderma* 124, 37–47.

Stevenson, B.A., Kelly, E.F., McDonald, E.V., Busacca, A.J., Welker, J.M., 2010. Oxygen isotope ratios in Holocene carbonates across a climatic gradient, eastern Washington State, USA: evidence for seasonal effects on pedogenic mineral isotopic composition. *The Holocene* 20, 575–583.

Sweeney, M.R., Busacca, A.J., Gaylord, D.R., 2005. Topographic and climatic influences on accelerated loess accumulation since the last glacial maximum in the Palouse, Pacific Northwest, USA. *Quaternary Research* 63, 261–273.

Sweeney, M.R., Busacca, A.J., Richardson, C.A., Blinnikov, M., McDonald, E.V., 2004. Glacial anticyclone recorded in Palouse loess of northwestern United States. *Geology* 32, 705–708.

https://doi.org/10.1017/qua.2018.47 Published online by Cambridge University Press

Sweeney, M.R., Gaylord, D.R., Busacca, A.J., 2007. Evolution of Eureka Flat: a dust-producing engine of the Palouse loess, USA. *Quaternary International* 162, 76–96.

Takeuchi, A., Goodwin, A.J., Moravec, B.G., Larson, P.B., Keller, C. K., 2009. Isotopic evidence for temporal variation in proportion of seasonal precipitation since the last glacial time in the inland Pacific Northwest of the USA. *Quaternary Research* 72, 198–206.

Thompson, R.S., Whitlock, C., Bartlein, P.J., Harrison, S.P., Spaulding, W.G., 1993. Climatic changes in the western United States since 18,000 yr BP. In: Wright, H.E., Jr., Kutzbach, J.E., Webb, T., III, Ruddiman, W.F., Alayne, S.-P.F., Bartlein, P.J. (Eds.), *Global Climates since the Last Glacial Maximum*. University of Minnesota Press, Minneapolis, MN, pp. 468–513.

Tobin, T.S., Schauer, A.J., Lewarch, E., 2011. Alteration of micromilled carbonate $\delta^{18}O$ during Kiel Device analysis. *Rapid Communications in Mass Spectrometry* 25, 2149–2152.

Waitt, R.B., 1985. Case for periodic, colossal jökulhlaups from Pleistocene glacial Lake Missoula. *Geological Society of America Bulletin* 96, 1271–1286.

Whitlock, C., Bartlein, P.J., 1997. Vegetation and climate change in northwest America during the past 125 ka. *Nature* 388, 57–61.

Whitlock, C., Bartlein, P.J., Markgraf, V., Ashworth, A.C., 2001. The midlatitudes of North and South America during the Last Glacial Maximum and early Holocene: similar paleoclimatic sequences despite differing large-scale controls. In: Markgraf, V., *Interhemispheric Climate Linkages: Present and Past Interhemispheric Climate Linkages in the Americas and their Societal Effects*. Academic, New York, pp. 391–416.

Williams, G.E., Polach, H.A., 1971. Radiocarbon dating of arid-zone calcareous paleosols. *Geological Society of America Bulletin* 82, 3069–3086.

Yang, W., Amundson, R., Trumbore, S., 1994. A model for soil $^{14}CO2$ and its implications for using ^{14}C to date pedogenic carbonate. *Geochimica et Cosmochimica Acta* 58, 393–399.

Zamanian, K., Pustovoytov, K., Kuzyakov, Y., 2016. Pedogenic carbonates: forms and formation processes. *Earth-Science Reviews* 157, 1–17.

https://doi.org/10.1017/qua.2018.47 Published online by Cambridge University Press